

AIAA
TP
91-3379



A91-44319

AIAA-91-3379

**Localization of Aeroelastic Modes in
Mistuned High-Energy Turbines**

Christophe Pierre

The University of Michigan

Ann Arbor, MI

and

Institute for Computational Mechanics in Propulsion

Lewis Research Center

Cleveland, OH

Todd E. Smith

Sverdrup Technology, Inc.

NASA Lewis Research Center Group

Brook Park, OH

Durbha V. Murthy

The University of Toledo

Toledo, OH

TP 91-3379

Y

**AIAA/SAE/ASME/ASEE
27th Joint Propulsion Conference
June 24-27, 1991 / Sacramento, CA**

NASA Technical Memorandum 104445
ICOMP-91-11; AIAA-91-3379

Localization of Aeroelastic Modes in Mistuned High-Energy Turbines

Christophe Pierre
The University of Michigan
Ann Arbor, Michigan

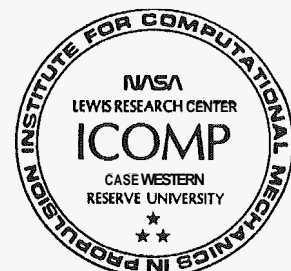
and

Institute for Computational Mechanics in Propulsion
Lewis Research Center
Cleveland, Ohio

Todd E. Smith
Sverdrup Technology, Inc.
NASA Lewis Research Center Group
Brook Park, Ohio

Durbha V. Murthy
The University of Toledo
Toledo, Ohio

Prepared for the
27th Joint Propulsion Conference
sponsored by the AIAA, SAE, ASME, and ASEE
Sacramento, California, June 24-27, 1991



LOCALIZATION OF AEROELASTIC MODES IN MISTUNED HIGH-ENERGY TURBINES

A91-44319

Christophe Pierre"
The University of Michigan
Department of Mechanical Engineering and Applied Mechanics
An Arbor, Michigan 48109
and
Institute for Computational Mechanics in Propulsion
Lewis research Center
Cleveland, Ohio 44135

Todd E. Smith
Sverdrup Technology, Inc.
Lewis Research Center Group
Brook Park, Ohio 44142

Durbha V. Murthy†
The University of Toledo
Department of Mechanical Engineering
Toledo, Ohio 43606

0. ABSTRACT

The effects of blade mistuning on the aeroelastic vibration characteristics of high-energy turbines are investigated, using the first stage of the oxidizer turbopump in the space shuttle main rocket engine as an example. A modal aeroelastic analysis procedure is used in concert with a linearized unsteady aerodynamic theory that accounts for the effects of blade thickness, camber and steady loading. Extreme sensitivity of the dynamic characteristics of mistuned rotors is demonstrated. In particular, the aeroelastic modes become localized to a few blades, possibly leading to rogue blade failure, and the locus of the aeroelastic eigenvalues loses its structure when small mistuning (of the order present in actual rotors) is introduced. Perturbation analyses that yield physical insights into these phenomena are presented. A powerful but easily calculated stochastic sensitivity measure that allows the global prediction of mistuning effects is developed.

1. INTRODUCTION

The current trend in the design of high performance propulsion turbomachinery has resulted in systems designed for finite service life. These systems produce high power, in compact and light-weight machines which require stringent safety factors and margins. In this environment, the design engineer is faced with the task of accurately predicting system performance and dynamics. When designing for specific life and reliability goals, the structural dynamic behaviors of the turbomachine are of paramount importance.

*Work funded by Space Act Agreement C-99066-G.

†NASA Resident Research Associate at Lewis Research Center.

The prediction of the dynamics of turbomachine rotors is further complicated by the presence of blade-to-blade differences in structural and material properties. These differences are unavoidable because they arise from manufacturing deviations and in-service degradation. They result in random blade-to-blade variations in natural frequencies, a phenomenon commonly referred to as frequency **mistuning**. Although most current analyses do not account for mistuning, mistuned rotors may exhibit dynamic characteristics that are vastly different from those assemblies with identical blades, termed tuned rotors.

In particular, previous studies have demonstrated that mistuning (a) increases the aeroelastic stability of rotors (Bendiksen, **1984**; Crawley and Hall, **1985**) and (b), results in larger forced response amplitudes (Ewins, **1973**; El-Bayoumi and Srinivasan, **1975**; Kielb and Kaza, **1984**). Furthermore, it has recently been shown that mistuning can alter the overall dynamics of rotors in a qualitative fashion. Namely, the equally distributed vibration amplitudes that characterize tuned rotors have been shown to become **localized** by mistuning to a few rotor blades, termed rogue blades (Pierre and Murthy, **1991**; Wei and Pierre, **1988a**; Valero and Bendiksen, **1986**). This has important implications in that the resulting energy confinement within a few blades indicates a possible cause for rogue blade failure in rotors.

In this paper we investigate the effects of blade mistuning on the aeroelastic vibration characteristics of a class of bladed-disk assemblies, namely high-energy turbines. The specific rotor we analyze is the first stage of turbine blades of the oxidizer turbopump (HPOTP) in the space shuttle main rocket engine (*SSME*). The *SSME* rotor was selected because it exhibits many of the characteristics of modern high performance turbomachinery designs. These include **high** energy density, low blade aspect ratio, high aerodynamic loading and advanced superalloy materials. In addition, the *SSME* turbopump turbines have been plagued with in-service blade failures during development and operational experience. These blades have suffered both low-cycle and high-cycle fatigue, which leads to the obvious presumption that significant dynamic loading exists. Contrary to previously suggested failure mechanisms (e.g., thermal shock), the present work proposes a theory which is based on the intrinsic dynamic characteristics of mistuned rotors.

The main results of our study are that rotors with characteristics similar to the *SSME* rotor are extremely sensitive to small mistuning and that their dynamics is qualitatively altered; for example, aeroelastic modes become **localized** to a few blades and the locus of the eigenvalues loses its structure when small mistuning is introduced.

The paper is organized as follows. Section 2 presents the structural and aerodynamic models and the formulation of the aeroelastic eigenvalue problem for high energy turbines. In Section 3 numerical results are presented for the *SSME* turbine with various levels of mistuning. Efficient perturbation methods that provide insight into mistuning effects are applied in Section 4. In Section 5 a stochastic sensitivity measure is developed that allows us to predict the sensitivity of bladed disk assemblies to random mistuning without having to solve mistuned aeroelastic eigenvalue problems. The

effectiveness of the sensitivity measure is illustrated by applying it to an advanced unshrouded fan stage. Finally, Section 6 concludes the paper.

There are two main contributions in this work. First, we show the extreme sensitivity to mistuning and the occurrence of localized vibrations for a full model of a **real** bladed-disk assembly, namely the **SSME** turbopump turbine. This has important implications for the **SSME** turbine in particular and high-energy turbines in general, because localized vibrations result in higher blade amplitudes and stresses and thus in shorter fatigue life and possibly rogue blade failure. Second, a **fundamental** contribution lies in the development of the powerful stochastic sensitivity measure, which allows for the global prediction of mistuning effects based solely upon tuned system information. The sensitivity measure is a generic tool that can be applied to any bladed-disk assembly.

2. AEROELASTIC FORMULATION

In this paper the bladed disk is modeled as a coupled system of N blades. Each blade's dynamics is described by a **single** in-vacuum (rotating) natural mode of vibration, say the n th natural mode. This simplified representation assumes that the coupling between the natural modes of an individual blade is negligible. Therefore, the rotor equations of motion are a system of N ordinary differential equations, each of which corresponds to an individual blade on the rotor. (Note that for the **SSME** turbopump turbine we developed a general formulation and a computer program that allow for interactions between various blade modes; however, we found that the blade natural frequencies for the **SSME** turbopump are so well separated that inter-mode coupling is insignificant; this justifies the single-mode per blade assumption.)

For simplicity, we assume that the blades are coupled only aerodynamically, and that there is **no structural coupling** of the blades through the disk or at the shrouds. Moreover, we are examining the aeroelastic free vibration of the assembly, and thus include in our model only those aerodynamic forces that are motion-dependent. The application of component mode analysis to the N -blade assembly yields a set of N homogeneous, linear, ordinary differential equations in the modal amplitudes of the blades. We look for motions such that all the blade coordinates oscillate with the same frequency and/or decay or grow at the same rate. This yields the following **aeroelastic** eigenvalue problem of order N :

$$(1) \quad [\lambda^2 \mathbf{M} + \mathbf{K} - \mathbf{A}(\omega_a)] \mathbf{u} = \mathbf{0}$$

where

- $\mathbf{u} = [u_1, u_2, \dots, u_N]^T$ is the complex eigenvector of the blade modal amplitudes, where T denotes a transpose
- \mathbf{M} and \mathbf{K} are the real inertia and stiffness matrices, respectively

– \mathbf{A} is the complex aerodynamic matrix, which depends on the assumed frequency, ω_a .

– λ is the complex eigenvalue

Since there is no structural coupling, the rotor mass and stiffness matrices are diagonal and of the form

$$(2) \quad \mathbf{M} = \mathbf{I}$$

$$(3) \quad \mathbf{K} = \text{diag}[\omega_{(n)1}^2, \omega_{(n)2}^2, \dots, \omega_{(n)N}^2]$$

where the blade modes have been normalized with a unit modal mass, and $\omega_{(n)j}$ is the n th natural frequency of the j th blade (rotating and in a vacuum). For a tuned assembly the diagonal elements of \mathbf{K} are identical and equal to $\omega_{(n)0}^2$, the nominal blade frequency squared, i.e., $\mathbf{K} = \omega_{(n)0}^2 \mathbf{I}$. For a mistuned rotor, the individual blade frequencies are generally distinct and the stiffness matrix is diagonal but not proportional to \mathbf{I} .

The aerodynamic coupling matrix \mathbf{A} is a fully populated complex matrix which is evaluated using the unsteady aerodynamic theory of Verdon and Caspar (1982, 1984). Verdon's method is employed to calculate the unsteady forces on the blades due to a particular natural mode of motion for a (tuned) cascade of identical blades. This results in a traveling wave representation of the aerodynamic forces for the tuned cascade. A detailed description of the unsteady force calculation using this theory is given by Smith (1990, 1991).

The transformation of the aerodynamic influence coefficients between traveling wave coordinates and individual blade, or physical coordinates is defined by

$$(4) \quad \mathbf{A} = \mathbf{E} \tilde{\mathbf{A}} \mathbf{E}^*$$

where $\tilde{\mathbf{A}}$, the aerodynamic matrix in traveling wave coordinates, is a diagonal matrix of complex elements

$$(5) \quad \tilde{\mathbf{A}} = \text{diag}[\tilde{A}_1, \tilde{A}_2, \dots, \tilde{A}_N]$$

The unitary transformation matrix \mathbf{E} is given by

$$(6) \quad \mathbf{E} = [\mathbf{e}_1, \dots, \mathbf{e}_j, \dots, \mathbf{e}_N]$$

where

$$(7) \quad \mathbf{e}_j = \frac{1}{\sqrt{N}} [1, e^{i\beta_j}, \dots, e^{i(N-1)\beta_j}]^T \quad \beta_j = \frac{2\pi}{N}(j-1) \quad j=1, \dots, N$$

where β_j is the **interblade phase angle**.

Note that an iterative procedure is required in order to solve the aeroelastic eigenvalue problem, Eq. (1), because the aerodynamic forces are dependent upon the frequency of vibration. First, a frequency of oscillation is assumed, and the corresponding aerodynamic matrix \mathbf{A} is calculated. The eigenvalue problem is then solved and the eigenvalue whose frequency is closest to the assumed frequency is used to recalculate the \mathbf{A} matrix. This iterative procedure is continued until the assumed frequency matches the natural frequency corresponding to one of the eigenvalues.

The solution of Eq. (1) consists of N pairs of eigenvalues and eigenvectors. For an eigensolution (λ, \mathbf{u}) , the blade assembly's motion is given by $\mathbf{u}e^{\lambda t}$. The real part of the eigenvalue, $\text{Re}(\lambda)$, determines the damping for the mode, while the imaginary part, $\text{Im}(\lambda)$, is the damped natural frequency of oscillations of the mode. Flutter in a mode occurs when the real part of the eigenvalue is greater than or equal to zero (and if the damped natural frequency of the mode equals the assumed frequency).

For a tuned assembly the matrix \mathbf{E} diagonalizes the aeroelastic problem, Eq. (1). This means that the eigenvectors of the system are the columns of \mathbf{E} , hence the aeroelastic mode shapes of the tuned assembly are the $\mathbf{e}_j, j=1, \dots, N$, given by Eq. (7). For a motion in the j th mode all blades vibrate with **equal** amplitudes but with a **constant phase difference** β_j between adjacent blades. We will refer to the modes of the tuned assembly as **constant interblade phase angle modes**. Physically, these normal mode motions are waves traveling through the assembly with a phase change β_j at each blade. To each backward traveling wave \mathbf{e}_j corresponds a forward traveling wave \mathbf{e}_{N-j+2} which has the same number of (traveling) nodal diameters. After diagonalization of Eq. (1) with the similarity transformation defined by \mathbf{E} , the aeroelastic eigenvalues of the tuned assembly are readily given by:

$$(8) \quad \lambda_{0j}^2 = \tilde{\mathbf{A}}_j - \omega_0^2 \quad j=1, \dots, N$$

where the subscript (n), representing the n th blade mode, is dropped for simplicity.

For a mistuned assembly the constant interblade phase angle vectors \mathbf{e}_j do not uncouple the system (1) and thus are not the aeroelastic modes. A numerical or a perturbation solution of the aeroelastic eigenvalue problem is then required. In this work, we assume **small random frequency mistuning**: the mode shape of each blade is identical, the natural frequency of each blade is a small deviation from the nominal blade frequency,

and the frequencies for the individual blades are **generated using** random numbers from a uniform probability distribution function. The modes of mistuned assemblies are studied in the following sections.

3. MODE LOCALIZATION AND LOSS OF EIGENSTRUCTURE IN THE SSME TURBOPUMP TURBINE

The first stage of the **SSME** turbopump is a rotor consisting of 78 blades equally spaced on the disk. A three-dimensional finite element model is used to calculate the first three free vibration natural frequencies and mode shapes of individual blades in a vacuum. In order to account for blade root flexibility, linear springs are included at the surfaces of the firtree lobes. Recall that structural coupling is not included in the model and that the blades are coupled solely through aerodynamic effects. The unsteady, motion-dependent aerodynamic forces are calculated from a two-dimensional, linearized, unsteady aerodynamic theory applied in axisymmetric strips along the airfoil span. No structural energy dissipation is included in the model. Figure 1 displays the finite element model of one HPOTP turbine blade, along with the first three natural frequencies. For details on the structural and aerodynamic models see Smith (1990, 1991).

We observe in Fig. 1 that the individual blade natural frequencies are well separated. Since the damping (both structural and aerodynamic) for this rotor is typically very small, the dynamic interactions between the various blade modes due to aerodynamic coupling is negligible. Thus it is reasonable to model each blade as a single-degree of freedom oscillator for a given natural mode.

We solved the aeroelastic eigenvalue problem for the tuned rotor and for random mistuning of various strengths. Mistuning was measured by its dimensionless standard deviation, ϵ , equal to the standard deviation of the squares of the blade natural frequencies divided by the square of the nominal natural frequency. We used a **single** mistuning pattern for all results. The first three blade modes were considered. For the tuned system, we found that most of the interblade phase angle modes in the second group of modes (corresponding to an edgewise motion of the blades) undergo flutter instability, i.e., have a positive real part of the eigenvalues. This instability can be removed easily by including small structural damping in the model (Smith, 1991). No flutter was found in the other groups. Therefore, we focused our investigation of the effects of mistuning on this second group of modes, because it is the least damped. In all the results presented, the eigenvalues are non-dimensionalized with respect to the square of the nominal blade frequency.

3.1 Scattering of the Root Locus

The root locus of the 78 aeroelastic eigenvalues in the edgewise mode group is displayed in Fig. 2 for various mistuning values. The imaginary part of the eigenvalues is plotted versus their real part. Note the regular pattern featured by the root locus of the

tuned assembly. As mistuning increases, the regularity of the root locus is gradually lost, and for very small mistuning of standard deviation 0.2% the locus consists of a constellation of eigenvalues with little discernible pattern. This qualitative change for very small mistuning indicates the **extreme sensitivity** of the aeroelastic dynamics of the HPOTP turbine to mistuning. Besides the loss of structure of the root locus, we note that mistuning causes a narrowing of the range of the real parts of the eigenvalues (representing damping) but a stretching of the root locus in the imaginary direction (frequency). In particular, we observe that the real part of the most unstable eigenvalue (that with the largest real part) decreases when mistuning is introduced, thereby confirming the well-known stabilizing effect of mistuning (Bendiksen, 1984; Pierre and Murthy, 1991).

3.2 Localization of Aeroelastic Mode Shapes

The high sensitivity to mistuning detected in the root locus plots is perhaps best illustrated by the changes in the corresponding mode shapes. Figure 3 displays the amplitude pattern of the most unstable aeroelastic mode shape for several mistuning values. As expected, the mode shape of the tuned rotor is a constant interblade phase angle mode and thus features identical amplitudes for all blades. When mistuning increases, the whole assembly ceases to participate in the motion and the vibration becomes confined to a few of the blades, i.e., the phenomenon of **mode localization** occurs. The sensitivity of the assembly dynamics to mistuning is extreme: even for a very small mistuning of 0.05% the blade amplitudes vary widely throughout the rotor, and for 1% mistuning only four blades participate in the motion to any significant degree! This indicates that the transition from constant interblade phase angle modes to localized modes is very rapid.

The localization of the mode shapes is also illustrated in Fig. 4, which includes phase information about the modes. Polar plots of the eigenvectors are shown in the complex plane (imaginary versus real part). Each dot on these plots represents the complex amplitude of one blade, where the distance from the origin to the dot is the real amplitude and the angle with the horizontal axis is the phase (not the interblade phase angle). Figure 4 displays the mode shape corresponding to the highest frequency eigenvalue (that with the largest imaginary part) for the mistuning values of Fig. 3. We note that for the tuned system the highest frequency mode is the one with zero interblade phase angle (this is coincidental), represented in the complex plane by 78 equal amplitudes and 78 phases equal to zero, hence by a single dot. As mistuning of standard deviation 0.01% is introduced, we observe a significant scatter in the blade amplitudes. Most blades vibrate with amplitudes close to 0.5 and only a few blades have amplitudes close to 1, indicating the onset of localization for the extremely small mistuning $\epsilon = 0.01\%$! Another interesting observation is that the phase angles are much less affected by mistuning than the amplitudes: all phase angles remain between 0 and, say, 20 degrees, a scatter much smaller than that of the amplitudes. Thus although substantial localization occurs, all blades still vibrate approximately in phase. This feature is largely lost when localization becomes severe, as shown by the plots for $\epsilon = 0.1\%$ to 1%. The phase angles then do not have a particular

pattern. We also note that the localization of the highest frequency mode in Fig. 4 is more severe than that of the most unstable mode in Fig. 3. For example, for $\varepsilon = 1\%$ the highest frequency mode features a single blade vibrating, versus four blades for the most unstable mode.

In order to illustrate further this dependence of localization on the mode number, Fig. 5 shows the amplitude patterns of four of the 78 aeroelastic mode shapes for a given mistuning strength: two modes at the extremes of the frequency cluster, namely the lowest and highest frequency modes, and two modes near the middle of the frequency cluster, the least and most stable modes. Observe that the modes with the extreme frequencies are substantially more localized than those near the middle of the frequency band, and hence they are more sensitive to mistuning.

The localization of aeroelastic mode shapes by mistuning has important practical consequences for the HPQTP turbine and possibly other high-energy turbines. **First**, it means that for such systems, most tuned aeroelastic calculations are probably invalid not only in a quantitative but in a **qualitative** sense as well. **Second**, strong mode localization appears to be unavoidable because its onset occurs for mistuning levels that are well below those resulting from typical manufacturing tolerances. For example, for the SSME turbine, testing of several hundred blades led to mistuning standard deviations ranging from 0.5% to 5% in the various mode groups, while the onset of localization, in the present analysis, is for $\varepsilon = 0.01\%$. **Third**, the localization of the aeroelastic modes is a potentially dangerous phenomenon, even though mistuning helps stabilize the rotor. This is because the vibrational energy is concentrated in a few of the blades rather than being distributed equally throughout the rotor. Hence a few blades of the mistuned rotor vibrate with much larger amplitudes than if the rotor were tuned, which results in larger stresses, shorter fatigue life, and possibly blade failure. Thus localization provides a plausible explanation for the occurrence of blade cracks and single blade failures (rogue blades). **Fourth**, although our results are only concerned with the free response of the HPQTP turbine, we expect its forced response to be affected by mistuning in a similar way and forced response localization to occur, because the response can be expressed as a combination of motions in the free aeroelastic modes. Such correspondence between free and forced response is indicated by studies of localization in simple models of structurally coupled mistuned assemblies (Wei and Pierre, 1988a, 1988b).

3.3 Transition from Extended to Localized Modes

We have seen in Fig. 3 that the transition from constant interblade phase angle (or extended) modes to localized modes is very rapid, occurring primarily between 0% and 0.5% mistuning. We also note in Fig. 3 that the region of localization of a mode (i.e., the location of the blades with the largest amplitudes) changes for every mistuning level, until severe localization is reached for $\varepsilon = 0.5\%$. This suggests that the transition from extended to localized modes is complex. In this section we examine this transition region.

Figure 6 displays the loci of the real parts of the ten most unstable eigenvalues versus mistuning strength. We observe the following. In the region from 0% to approximately 0.05% mistuning, the variation of the eigenvalue real parts appears to be nearly parabolic, with all eigenvalues being affected by mistuning in a similar way. This parabolic variation, as opposed to a linear one, indicates the high sensitivity to mistuning. It suggests the use of second-order perturbation methods to capture this high sensitivity (see Section 4). In this parabolic region the mistuned system behaves as a perturbation of a tuned assembly, such that the structure of the root locus is nearly regular and the mode shapes feature similar amplitudes for all blades.

Figures 2 and 3 show that the tuned system characteristics begin to break down for $\varepsilon=0.05\%$. From $\varepsilon=0.05\%$ to 0.5%, we observe in Fig. 6 a region where the behavior of the eigenvalues exhibits great complexity. We label this zone the transition region. It is characterized by what appear to be numerous crossings of the loci of the eigenvalue real parts. The irregular shape of the lower envelope of these eigenvalue loci is due to the existence of crossings with the other eigenvalues of the system, which are not shown in Fig. 6.

Although Fig. 6 seems to display eigenvalue crossings, several studies of mode localization in other mistuned periodic systems [e.g., multi-span beams and chains of oscillators (Pierre, 1988)] have shown that eigenvalue loci typically do not cross, but veer away from each other abruptly. Distinguishing between veerings and crossings is difficult unless analytical solutions are available. In the present problem, although we decreased the mistuning increment close to machine accuracy, we were unable to prove that there is a nonzero minimum distance between two eigenvalue loci at their junction. Thus we were unable to determine whether veerings or crossings are displayed in Fig. 6. For definiteness we refer to those as “crossings” in the following.

The behavior of the eigenvectors near the eigenvalue loci crossings is of interest. In order to illustrate the change in the mode shapes through a crossing, we selected a nearly simultaneous crossing of three eigenvalue loci in Fig. 6. This triple crossing is displayed in Fig. 7, along with the corresponding mode shapes before and after the crossing.

First, we note that an enlargement of more than two order of magnitudes in mistuning was necessary in order to capture the crossing. This underlines the complexity of the dynamics in the transition region. Second, we observe from Fig. 7 that the modes simply switch positions before and after the crossing, i.e., each mode shape is clearly associated with an eigenvalue loci (here nearly a straight line) throughout the crossing region. Thus, if we choose to follow a given eigenvalue locus, the character of the associated mode is preserved through the crossing. However, if we choose to track, for example, the mode with the largest real part (the most unstable mode), this mode changes character every time it goes through a crossing. Since there are numerous crossings in the transition region, we can expect a mode shape to undergo numerous changes as mistuning increases. This is consistent with the observation made above in Fig. 3, which shows that

the most unstable mode becomes localized at various locations on the rotor as mistuning increases. These changes in the localization region correspond to the crossings with other eigenvalues.

The most striking feature of the transition region is its complexity (recall that only ten of the **78** eigenvalues are displayed in Fig. 6). Although the bladed disk considered is a **linear** system, it is apparent from Figs. 6 and 7 that its dynamics is extremely complicated for this range of mistuning, because the mode shapes and eigenvalues are greatly affected by small changes in the mistuning. For example, numerous mode switchings occur. Thus, in practice, it is difficult to **predict** accurately the modes of assemblies operating in the transition region.

For mistuning greater than 0.596, the transition to localized modes is nearly complete (see the mode shapes in Fig. 3). This localization region is characterized by fewer eigenvalue loci crossings than in the transition region, and by nearly **linear** variations of these loci with mistuning. This linear variation is due to the fact that the localized modes can be approximately associated with single decoupled blades, the frequency of which varies linearly with small mistuning (see the perturbation analysis in Section 4). This is in contrast with the region of very small mistuning, which features the high sensitivity associated with parabolic variation.

Figure 8 displays the imaginary parts (frequencies) of the ten lowest frequency eigenvalues versus mistuning. The same features as in Fig. 6 are present; as mistuning increases from zero, we encounter first a narrow region of extended modes, then a complex transition region where numerous frequency crossings occur, and finally a localization region where the frequencies vary nearly linearly with mistuning. Note, however, that the transition region for these ten lowest frequencies is much narrower than in Fig. 6 for the ten most unstable modes. This confirms the fact, observed in Fig. 5, that modes near the extremes of the frequency cluster (e.g., the low frequency ones) are more sensitive than those near the middle of the cluster (e.g., the most unstable ones), and that localization occurs first for the former.

Our results for the NPOTP turbine indicate that severe localization occurs at the mistuning levels measured for the **SSME** blades (typically between 1% and 4%), and that no modes belong to the transition region. However, structural coupling through the disk or tip shrouds would lower the sensitivity to mistuning and thus extend the transition region. Therefore it is conceivable that some of the modes of the real HPOTP rotor belong to the transition region and, although very different from extended modes, are not fully localized to a few blades. Moreover, other high-energy turbines may have different parameter values (interblade coupling, number of blades, blade stiffness, etc.) and thus may feature modes in the transition region. These modes would be difficult to predict accurately, as discussed above.

3.4 Localization of Various Mode Groups

The aeroelastic modes of the N -blade assembly are clustered in groups of N modes, such that each group corresponds to a blade mode. While the results given above focus on the effects of mistuning on the second mode group, it is of interest to compare the sensitivity of the other groups of blade modes and their localization.

The first three normal modes of the HPOTP turbine blade are bending, edgewise, and torsion, respectively. Figure 9 displays the amplitude patterns of the most unstable mode of the assembly in each group. The frequency mistuning pattern, as well as the mistuning strength of 0.5%, are taken to be identical for all three mode groups. We observe in Fig. 9 that although the bending mode is substantially affected by mistuning, it does not become localized. On the other hand, the modes in the edgewise and torsion groups become strongly localized, the latter slightly more than the former. Thus, the bending mode group is much less sensitive to mistuning than the edgewise and torsional mode groups, which feature nearly the same sensitivity. This behavior is explained in the next section.

4. PERTURBATION ANALYSES

In this section we seek an understanding of the physical mechanisms that govern the dynamics of mistuned assemblies. To that end, we have developed perturbation schemes that predict the high sensitivity to mistuning as well as characterize the degree of localization of the modes. Here we apply this perturbation approach to the HPOTP turbine. For details on the perturbation analyses, see Pierre and Murthy (1991)

4.1 Classical Perturbation Approach

The most natural perturbation procedure to study the dynamics of a mistuned assembly is one that considers the tuned assembly as the unperturbed system and the blade mistuning as the small perturbation. This approach, which we refer to as the classical method, yields easily eigenvalue and eigenvector perturbations to any order in the mistuning (first- and second-order results are given below). However, this classical approach is inherently flawed in cases of high sensitivity and localization. This is because choosing the small mistuning as the perturbation parameter requires the eigensolution of the mistuned assembly to be a small perturbation of that of the tuned assembly. Clearly, this is not the case when the phenomena of mode localization and root locus scattering occur, since in this case mistuning causes qualitative (i.e., very large) alterations in the assembly's dynamics. Thus, the classical perturbation analysis cannot capture the drastic changes in the dynamics caused by small mistuning. As we discuss below, however, the mere fact that the technique fails in the presence of localization can be used to predict the high sensitivity to mistuning.

Let us now explore the mechanisms of failure of the classical perturbation method. We denote the unperturbed stiffness matrix of the tuned assembly by \mathbf{K}_0 and the perturbation matrix due to small mistuning by $\delta\mathbf{K}$, where the latter is a diagonal matrix of mistunings in the squares of the individual blade frequencies, $\delta\omega_i^2$, such that $\delta\omega_i / \omega_0 \ll 1$ for $i=1, \dots, N$. The stiffness matrix of the perturbed (mistuned) assembly is therefore $\mathbf{K} = \mathbf{K}_0 + \delta\mathbf{K}$. The modes of the unperturbed system are the interblade phase angle modes given by Eqs. (7) and (8). Those of the perturbed system can be expanded in a perturbation series as

$$(9) \quad \left. \begin{aligned} \lambda_i &= \lambda_{0i}^2 + \delta\lambda_i^2 + \delta^2\lambda_i^2 \\ \mathbf{u}_i &= \mathbf{e}_i + \delta\mathbf{u}_i + \delta^2\mathbf{u}_i \end{aligned} \right\} \quad i = 1, \dots, N$$

where $\delta\lambda_i^2$ and $\delta\mathbf{u}_i$ (respectively $\delta^2\lambda_i^2$ and $\delta^2\mathbf{u}_i$) are first-order (respectively second-order) terms in the small mistuning.

Applying perturbation theory to the eigenvalue problem (Courant and Hilbert, 1953), one can show that the first-order perturbation of the eigenvalues is

$$(10) \quad \delta\lambda_i^2 = -\frac{1}{N} \sum_{k=1}^N \delta\omega_k^2 \quad i = 1, \dots, N$$

We readily observe that for small mistuning this is always a small term. Hence the first-order eigenvalue perturbation **cannot** reveal high sensitivity to mistuning. Moreover, all eigenvalues are shifted by an **identical** amount and, for a mistuning pattern that averages to zero, the change in the eigenvalues equals zero. Another interesting remark is that the perturbation of the eigenvalue squared is real, therefore mistuning, to the first-order, does not affect the stability of the assembly (or very little). Here we reach the seemingly contradictory conclusion that if the average mistuning throughout the rotor is not zero, **i.e.**, if we stiffen or soften **all** the blades on the average, the flutter boundary remains unchanged! The explanation of this paradox lies in the fact that the assumed frequency that was used for the aerodynamic computations is then no longer valid. If the effect of mistuning with nonzero mean on flutter is sought, the full mistuned eigenvalue problem must be solved in order to determine the correct assumed frequency. These remarks suggest that, although simple and cost-effective, perturbation methods must be used with care in a design environment.

Returning to our main discussion, we now give the second-order perturbation of the eigenvalues:

$$(11) \quad \delta^2 \lambda_i^2 = \sum_{\substack{k=1 \\ k \neq i}}^N \frac{|\mathbf{e}_k^* \delta \mathbf{K} \mathbf{e}_i|^2}{\lambda_{0i}^2 - \lambda_{0k}^2} = \sum_{\substack{k=1 \\ k \neq i}}^N \frac{|\mathbf{e}_k^* \delta \mathbf{K} \mathbf{e}_i|^2}{\tilde{\mathbf{A}}_i - \tilde{\mathbf{A}}_k} \quad i = 1, \dots, N$$

where $*$ denotes complex conjugate and $|\cdot|$ the modulus of a complex quantity. In Eq. (11), the numerator in the summation is a measure of the square of the mistuning (in the frequency squares), and the denominator is the spread among the interblade phase angle aerodynamic coefficients. For the HPOTP turbopump, these aerodynamic coefficients are small because the unsteady aerodynamic forces are small compared to elastic and inertia forces and provide **very weak coupling between the blades**. Equation (8) shows that the spread in the interblade phase angle aerodynamic coefficients is simply that in the tuned aeroelastic eigenvalues. From Fig. 2, this spread is seen to be about four orders of magnitude smaller than the square of the nominal blade frequency. Thus, if mistuning is of the order of, say 1%, the numerators and denominators in Eq. (11) are of comparable magnitudes and the second-order eigenvalue perturbation is of the order of **one**, not second order. The fact that eigenvalue perturbations become large indicates the failure of the perturbation analysis and reveals the **high sensitivity** of the assembly dynamics to mistuning.

Several remarks are in order. **First**, the above discussion examines a single term in the summation, Eq. (11). Multiple terms in the summation generally increase the magnitude of second-order perturbation. Thus we expect the sensitivity to mistuning to increase with the number of blades (this is discussed in Section 5). **Second**, although not shown here, the aeroelastic eigenvector perturbations behave similarly to the second-order eigenvalue perturbations, i.e., the sensitivity of the eigenvectors is inversely proportional to the aerodynamic coefficients. This is consistent with the drastic alterations of the mode shapes observed in Fig. 3. **Third**, although the failure of the perturbation analysis indicates high sensitivity to mistuning, the perturbation results **cannot** be used to characterize the behavior of the mistuned assembly, as they are qualitatively in error. **Fourth**, a classical perturbation analysis does not always fail. For example, if mistuning is extremely weak, e.g., 0.01% for the SSME turbopump, the ratios in Eq. (11) may be sufficiently small for the perturbation expression to be valid. This is also the case if the interblade coupling is strong, such that the aerodynamic coefficients, and thus the denominators in Eq. (11) are not small. In these cases mistuning has a small effect on the assembly's dynamics.

We now have an understanding **of** the mechanism for high sensitivity to mistuning. It is the closeness of the aeroelastic eigenvalues of the tuned assembly that determines how sensitive the assembly is. This spread in the eigenvalues is governed by the magnitude of the aerodynamic coefficients, and therefore by the strength of the aerodynamic interblade coupling (see Eqs. (8) and (11)). This mechanism is the same as that identified for assemblies with structural interblade coupling (Wei and Pierre, 1988a). In the case of the HPOTP turbine the interblade coupling is very weak and thus the tuned aeroelastic

eigenvalues are very close, which results in an extreme sensitivity to mistuning, as shown by the results in Section 3.

For example, we can use the closeness of the tuned eigenvalues to predict the sensitivity in the various groups of modes. For the first group of modes (bending), we found that the spread in the imaginary parts (the frequencies) of the tuned eigenvalues is approximately 0.004%, while the corresponding spread for the second group of modes (edgewise) is only 0.001%. This means, since the distance between eigenvalues is governed by the strength of aerodynamic effects, that the interblade coupling is weaker for the edgewise modes than for the bending modes. Accordingly, the edgewise modes feature a much higher sensitivity to mistuning than the bending modes, as shown by the localization displayed in Fig. 9.

4.2 Modified Perturbation Method

While identifying the cause of high sensitivity is useful, it does not provide answers regarding the behavior of the mistuned assembly, viz. the occurrence of mode localization. In order to characterize the dynamics of mistuned assemblies, we have developed a modified perturbation approach described below.

The key idea behind the modified perturbation scheme is to recognize that high sensitivity is caused by small interblade coupling and hence **the interblade coupling ought to be treated as a perturbation**. With this approach, the (modified) unperturbed system is purely structural, consisting of uncoupled mistuned blades in a vacuum. It thus has distinct natural frequencies (unless two or more blades happen to have the same frequencies, but we do not consider this case here). The (modified) perturbation consists of the small unsteady aerodynamic forces, which provide the interblade coupling. Each normal mode of the unperturbed system features uncoupled oscillations of a single mistuned blade, with all others remaining quiescent. When weak aerodynamic interblade coupling is introduced, the neighboring blades participate in the motion, but do so with small amplitudes because the small coupling is not sufficient to cause a resonance among the slightly different blades. Each mode of the mistuned assembly is a perturbation of the oscillations of a single blade, and thus is localized to that blade or to a small group of blades around it, depending upon the relative magnitudes of the coupling and the mistuning. Examples of localized modes are given in Fig. 3. In summary, the modified perturbation method simply utilizes the fact that, for weak enough interblade coupling or strong enough blade mistuning, the modes of the mistuned assembly are perturbations of the modes of the decoupled mistuned assembly, i.e., of single blade oscillations.

The modified perturbation scheme can be easily implemented by treating the aerodynamic matrix in Eq. (1) as the perturbation; for details see Pierre and Murthy (1991). The mistuned assembly eigenvalues are given by, to the second-order in the interblade coupling:

$$(12) \quad \lambda_i^2 = -(\omega_i^2 + \delta\omega_i^2) + A, - \sum_{\substack{k=1 \\ k \neq i}}^N \frac{A_{ki}A_{ik}}{\delta\omega_i^2 - \delta\omega_k^2} + \text{H.O.T.}$$

where the zeroth-, first-, and second-order terms in the interblade coupling are the first three terms on the right-hand-side, respectively. Clearly, the effect of the aerodynamic coupling is to modify slightly the assembly eigenvalues from the individual blade frequencies. Also, the second-order term in Eq. (12) indicates that the modified perturbation approach fails when mistuning is too small.

4.3 Validity of the Perturbation Schemes

Figure 10 displays the percentage error between the “exact” numerical eigensolution and the two perturbation results versus the strength of mistuning, for the imaginary part of the lowest frequency eigenvalue. We note that for very small mistuning the classical perturbation result agrees well with the exact solution, such that in this region the mistuned assembly behaves as a perturbation of the tuned one. This corresponds to the region of parabolic variation of the eigenvalues in Fig. 8. As mistuning increases the classical perturbation result diverges rapidly from the exact solution, while the modified perturbation approximation approaches the exact solution. This second zone, where neither perturbation scheme provides a good approximation of the eigensolution, corresponds to the complex transition region. Finally, as mistuning increases to 0.5%, the agreement between the exact and modified perturbation solutions becomes nearly perfect. In this case the mistuned assembly behaves as a perturbation of an assembly of decoupled blades. This corresponds to the localization region characterized by straight eigenvalue loci in Fig. 8. Finally, note that the error of the appropriate perturbation schemes is never greater than 0.05%. This makes the cost-effective perturbation methods accurate analysis and design tools.

As an example of mistuned assembly dynamics prediction, Fig. 11 displays the root locus of the eigenvalues of the HPOTP assembly with 2% mistuning, by both the modified perturbation scheme and the exact solution procedure. The perturbation method clearly captures the features of the root locus, both qualitatively and quantitatively. For example, the scattering of the locus, as opposed to the regular structure of the tuned locus, is reproduced by the perturbation result. We also note that the exact frequencies (the imaginary parts) are closely matched by the perturbation results. Larger discrepancies occur for the real parts (the damping values) and we believe this is due to the fact that damping is small for all the modes. Finally, we note that one of the eigenvalues (or at least its real part) is not predicted accurately by the perturbation method. We believe this occurs because, in the random mistuning pattern used, two neighboring blades have nearly equal mistuned natural frequencies. In this case the modified perturbation approach fails, see Eq. (12).

5. A STOCHASTIC MEASURE OF SENSITIVITY

The perturbation schemes discussed above provide a physical understanding of the sensitivity to mistuning and allow for the analysis of localized modes. In this section we develop a sensitivity measure that will allow the designer to predict, in a very simple way, the effects of mistuning on the various aeroelastic modes. Because mistuning is random in nature, a statistical approach is chosen to obtain a compact measure of sensitivity. This measure allows us to predict mistuning effects essentially with a single scalar for each mode. However, a possible drawback of this stochastic measure is that **individual realizations** of mistuning patterns may result in dynamic behaviors much different from the **average** behavior predicted by the sensitivity measure (for example, a “sinusoidal” mistuning pattern alters the dynamics much less than a truly random pattern).

The sensitivity measure defined below does not require the mistuned system solution and thus is cost effective. Moreover, since the forced response of mistuned assemblies consists of linear combination of responses in the free modes of vibration, the sensitivity of the aeroelastic modes will provide useful information about that of the forced response. Thus, this measure has the potential to become a valuable design tool.

5.1 Theoretical Development

The basic idea is to define the sensitivity of the system by taking the statistical average of the second-order eigenvalue perturbation (here mistuning is the perturbation). This is motivated by the findings in Section 4, which showed that the mechanism for high sensitivity, i.e., the closeness of the tuned eigenvalues, is embedded in the second-order perturbation, while the first-order perturbation always remains small. We rewrite Eq. (11) using the expression for the interblade phase angle mode shapes, \mathbf{e}_j , given in Eq. (7). After some algebra, we obtain:

$$(13) \quad \delta^2(\lambda_i^2) = - \sum_{\substack{k=1 \\ k \neq i}}^N \frac{1}{\tilde{\mathbf{A}}_k - \tilde{\mathbf{A}}_i} \left[\sum_p \delta\omega_p^2 + \sum_{\substack{p,q \\ p \neq q}} \cos\left(\frac{2\pi}{N}(i-k)(p-q)\right) \delta\omega_p^2 \delta\omega_q^2 \right]$$

At this point we need to define the mistunings in the frequency squared, $\delta\omega_p^2$, $p=1, \dots, N$, as independent and identical random variables of mean zero and standard deviation, σ . This simply means that the blades are chosen randomly from an (ideally) infinite population. Next we take the statistical average, over the random mistunings, of the second-order eigenvalue perturbation. This simply yields

$$(14) \quad \langle \delta^2(\lambda_i^2) \rangle = - \sum_{\substack{k=1 \\ k \neq i}}^N \frac{1}{\tilde{\mathbf{A}}_k - \tilde{\mathbf{A}}_i} N \sigma^2 \quad i = 1, \dots, N$$

because $\langle (\delta\omega_p)^2 \rangle = \sigma^2$ and, for $p \neq q$, $\langle \delta\omega_p \delta\omega_q \rangle = 0$, where $\langle \cdot \rangle$ denotes an average.

Now consider the Taylor expansion of the i th eigenvalue in terms of mistuning, **Eq. (9)**, and take its statistical average. Since the first-order perturbation is proportional to mistuning, it averages to zero and we obtain

$$(15) \quad \langle \lambda_i^2 \rangle = \lambda_{0i}^2 - \sum_{\substack{k=1 \\ k \neq i}}^N \frac{1}{\tilde{\mathbf{A}}_k - \tilde{\mathbf{A}}_i} N \sigma^2 \quad i = 1, \dots, N$$

This shows that to the second order, the locus of the average of an eigenvalue versus the mistuning standard deviation is a parabola. The curvature of this parabola determines the sensitivity of the associated aeroelastic mode to mistuning. Hence we rewrite

$$(16) \quad \langle \lambda_i^2 \rangle = \lambda_{0i}^2 + S_i \sigma^2 \quad i = 1, \dots, N$$

where we have defined the **stochastic sensitivity measure** of the i th eigenmode to mistuning as

$$(17) \quad S_i = - \left(\sum_{\substack{k=1 \\ k \neq i}}^N \frac{1}{\tilde{\mathbf{A}}_k - \tilde{\mathbf{A}}_i} \right) N \quad i = 1, \dots, N$$

We say a mode features a low, or normal sensitivity when the expansion **(16)** is valid. This occurs when the term $S_i \sigma^2$ is second-order and therefore when the sensitivity measure S_i is of the order of one. High sensitivity in a mode occurs when $S_i \sigma^2$ is first-order or larger, implying the failure of the perturbation analysis. This happens when S_i is large.

In order to interpret results it is useful to make our sensitivity measure dimensionless. This is achieved first by expressing S_i in terms of the dimensionless mistuning standard deviation ε , where $\varepsilon = \sigma/\omega_0^2$. The second step is to divide S_i by a representative eigenvalue of the system, such that all sensitivities are referred to **1** rather than to the various λ_{0i}^2 . Here we choose to nondimensionalize S_i by the eigenvalue

corresponding to the tuned blade frequency squared, $-\omega_0^2$ (ideally we should divide by λ_{0i}^2 given in Eq. (8) but this would result in a complicated expression for S_i ; moreover, for small aerodynamic coefficients, these two normalizations are nearly equivalent). The selected normalization yields the dimensionless sensitivity measure:

$$(18) \quad \bar{S}_i = \left(\sum_{k \neq i} \frac{\omega_0^2}{\tilde{\mathbf{A}}_k - \tilde{\mathbf{A}}_i} \right) N \quad i = 1, \dots, N$$

From Eq. (18), we observe readily that the sensitivity measure increases as the aerodynamic interblade coupling decreases and as the number of blades increases. Detailed results are given below.

5.2 Sensitivity Results

Here we use our stochastic sensitivity measure in order to reach general results regarding mistuning effects. Note that \bar{S}_i is a complex number that characterizes the sensitivity of both the frequency and damping of a tuned mode to mistuning. The damping in a mode, however, is always small (this does not mean it is unimportant) and we have consistently observed that the sensitivity of the frequency is the one that governs mistuning effects. Hence we focus on the real part of our sensitivity measure.

Since the computation of aerodynamic forces for the SSME turbine is expensive, we used another blade assembly to investigate the effectiveness of \bar{S}_i in predicting high sensitivity and localization. This rotor is an advanced unshrouded fan stage, studied earlier by Pierre and Murthy (1991) and Kaza and Kielb (1984). Complete details about the models and the rotor properties can be obtained from the above references.

Figure 12 displays the real part (representing frequency) of the sensitivity of the modes of a 78-bladed rotor. The eigenvalues are sorted from the lowest frequency tuned mode to the highest frequency one. The sensitivities of all the modes are very large (much larger than 1; note the scale). This predicted high sensitivity is confirmed by the lowest frequency mode of the 78-blade rotor, displayed in Fig. 13 for $\varepsilon=0.63\%$. This mode exhibits strong localization features. Moreover, Fig. 12 shows that the modes with the lowest and the highest frequencies are much more sensitive to mistuning than those near the middle of the frequency cluster. This is fully consistent with the results presented in Fig. 5 for the SSME turbine, which showed that the least and most stable modes (typically located near the middle of the mode group) are less severely localized than the lowest and highest frequency modes.

Figure 13 displays the lowest frequency mode of this rotor for various numbers of blades, from $N=20$ to $N=78$. We note that while the mode of the 20-blade assembly is

localized to approximately one-half the blades on the rotor, the degree of localization of the same mode increases rapidly with the number of blades. For the 78-blade rotor only one-sixth of the blades participate significantly in the motion.

The sensitivity measure of the real part (frequency) of the lowest frequency mode is plotted in Fig. 14 versus the number of blades in the rotor. (The sensitivity is negative because the lowest frequency is decreased by the introduction of mistuning.) We note that, in absolute value, the sensitivity measure increases rapidly with the number of blades, thereby confirming the localization results shown in Fig. 13. (Note that the sensitivities for small numbers of blades are not small, but only appear so because of the large scale.)

On a final note, we point out that the calculation of the sensitivities for all the modes is a trivial task that requires only the tuned assembly's eigensolution. No solution of the mistuned eigenvalue problem is required. This sensitivity measure could be used effectively as a design tool.

6. CONCLUDING REMARKS

The main finding of this study is that the aeroelastic characteristics of high-energy turbines can be highly sensitive to small random blade mistuning. Weak aerodynamic coupling between blades is the cause of this sensitivity. As an application, the aeroelastic modes of the SSME HPOTP turbine were examined.

Upon introduction of small mistuning, the root locus of the aeroelastic eigenvalues loses the regular structure that characterizes the tuned assembly to become randomly scattered, and the constant interblade phase angle mode shapes of the tuned assembly become strongly localized to a few of the blades. The occurrence of vibration localization has important consequences for high-energy turbines. Localization results in a confinement of vibrational energy to a few of the blades, and therefore in a possibly large increase in amplitude for those blades. In turn, stresses are larger and fatigue life is shorter, which can ultimately result in the failure of those few blades.

We did not consider structural coupling, either through the disk or tip shrouds, in our study. However, previous research (Wei and Pierre, 1988a; Pierre and Murthy, 1991) has shown that aerodynamic and structural coupling affect the sensitivity to mistuning in the same qualitative fashion. Hence, including structural coupling in our model would increase interblade coupling and lower the sensitivity to mistuning. Let us consider an extreme situation where the structural coupling is ten times stronger than the aerodynamic one. Since the degree of localization is a function of the ratio of coupling to mistuning (Pierre, 1988), the assembly with both aerodynamic and structural couplings requires a mistuning ten times larger than that for the aerodynamic-only system in order to produce the same localization. For the SSME, since 0.1% mistuning causes strong localization in the

aerodynamic-only system, it means that a mistuning of 1% would be needed. With mistuning estimates typically ranging from 1 to 5%, we conclude that high sensitivity and strong localization would still be observed in this extreme situation. The study of mistuned assemblies with both structural and aerodynamic interblade coupling will be the subject of future research.

Although our study focused on the free response of blade assemblies, the forced response problem is of greater interest to the turbine designer. The next step in our research is to examine mistuning effects on the forced response. We conjecture that high sensitivity to mistuning and vibration localization also occur for the forced response of mistuned assemblies. This is based on two reasons. The first is that previous studies of localization in simple models of structurally coupled assemblies have shown that both free and forced responses feature localized vibration patterns (Wei and Pierre, 1988a, 1988b). The second reason is that the forced response, through modal analysis, is expressed as a linear combination of responses in the free modes, and thus retains the key features of the free dynamics of the assembly, especially near resonances. This is in fact why a thorough understanding of the free response is necessary before tackling the forced response problem.

The perturbation techniques and the sensitivity measure introduced in the paper, besides providing a physical understanding of mistuning effects, are cost-effective and have the potential to become useful tools for the turbine designer.

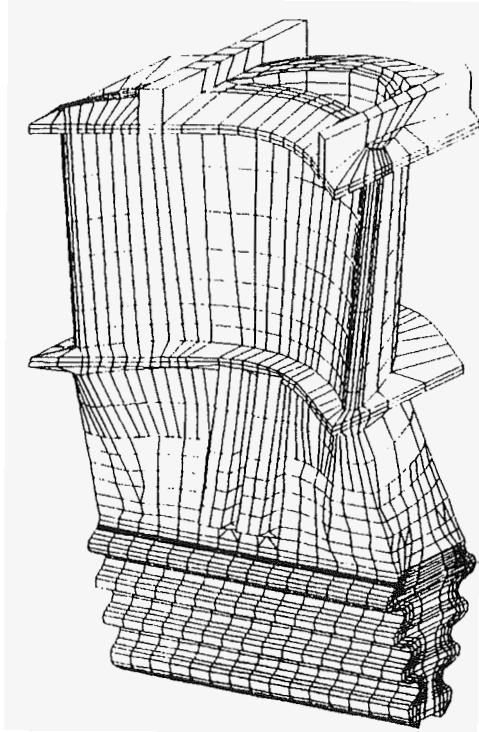
Finally, the pattern of blade mistuning along the assembly can strongly affect the localization of the aeroelastic modes. Based on our modified perturbation analysis, we conjecture that a “maximum randomness” in the mistuning pattern causes the most extreme localization. Conversely, “smooth” mistuning (e.g., a sinusoidal pattern) will probably lessen the strength of localization and tend to distribute energy among all blades. This suggests that it may be possible to **optimize** mistuning patterns to reduce localization and sensitivity to mistuning. If simple enough, such a system could be implemented in the manufacturing process **of** the assembly.

ACKNOWLEDGMENT

This work was supported by the Institute for Computational Mechanics in Propulsion and by NASA Lewis **Research Center** through grants NAG3-1163 and NAG3-742 and contract NAS3-25266. George Stefko was the technical monitor.

REFERENCES

- O. O. Bendiksen 1984 *ASME Journal of Engineering for Gas Turbine and Power* **106**, 25-33. Flutter of mistuned turbomachinery rotors.
- R. Courant and D. Hilbert 1953 *Methods of Mathematical Physics, Volume 1*. Interscience publishers: New York.
- E. F. Crawley and K. C. Hall 1985 *ASME Journal of Engineering for Gas Turbine and Power* **107**, 418-426. Optimization and mechanisms of mistuning in cascades.
- L. E. El-Bayoumy and A. V. Srinivasan 1975 *AIAA Journal* **13**, 460-464. Influence of mistuning on rotor-blade vibrations.
- D. J. Ewins 1973 *Journal of Mechanical Engineering Science* **15**, 165-186. Vibration characteristics of bladed disc assemblies
- K. R. V. Kaza and R. E. Kielb 1984 *AIAA Journal* **22**, 1618-1625. Flutter of turbofan rotors with mistuned blades.
- R. E. Kielb and K. R. V. Kaza 1984 *ASME Journal of Engineering for Gas Turbine and Power* **106**, 17-24. Effects of structural coupling on mistuned cascade flutter and response.
- C. Pierre 1988 *Journal of Sound and Vibration* **126**, 485-502. Mode localization and eigenvalue loci veering phenomena in disordered structures.
- C. Pierre and D. V. Murthy 1991 *AIAA Paper 91-1218*. Aeroelastic modal characteristics of mistuned blade assemblies: mode localization and loss of eigenstructure.
- T. E. Smith 1990 *AIAA Paper 90-2351*. Aeroelastic stability analysis of a high-energy turbine blade.
- T. E. Smith 1991 NASA Contractor Report 187089. A modal aeroelastic analysis scheme for turbomachinery blading.
- N. A. Valero and O. O. Bendiksen 1986 *ASME Journal of Engineering for Gas Turbine and Power* **108**, 293-299. Vibration characteristics of mistuned shrouded blade assemblies.
- J. M. Verdon and J. R. Caspar 1982 *AIAA Journal* **20**, 1259-1267. Development of a linear unsteady aerodynamic analysis for finite-deflection subsonic cascades.
- J. M. Verdon and J. R. Caspar 1984 *Journal of Fluid Mechanics* **149**, 403-429. A linearized unsteady aerodynamic analysis for transonic cascades.
- S. T. Wei and C. Pierre 1988a *ASME Journal of Vibration, Acoustics, Stress, and Reliability in Design* **110**, 429-438. Localization phenomena in mistuned assemblies with cyclic symmetry. Part I: free vibrations.
- S. T. Wei and C. Pierre 1988b *ASME Journal of Vibration, Acoustics, Stress, and Reliability in Design* **110**, 439-449. Localization phenomena in mistuned assemblies with cyclic symmetry. Part II: forced vibrations.



Mode 1 (Bending)	4748 Hz
Mode 2 (Edgewise)	9950 Hz
Mode 3 (Torsion)	16580 Hz

Figure 1. SSME HPOTP turbine blade finite element model and natural frequencies.

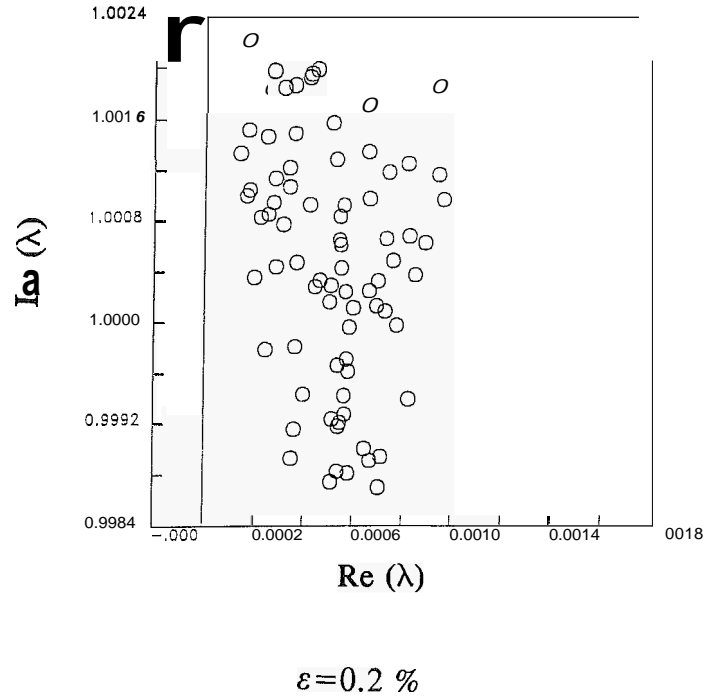
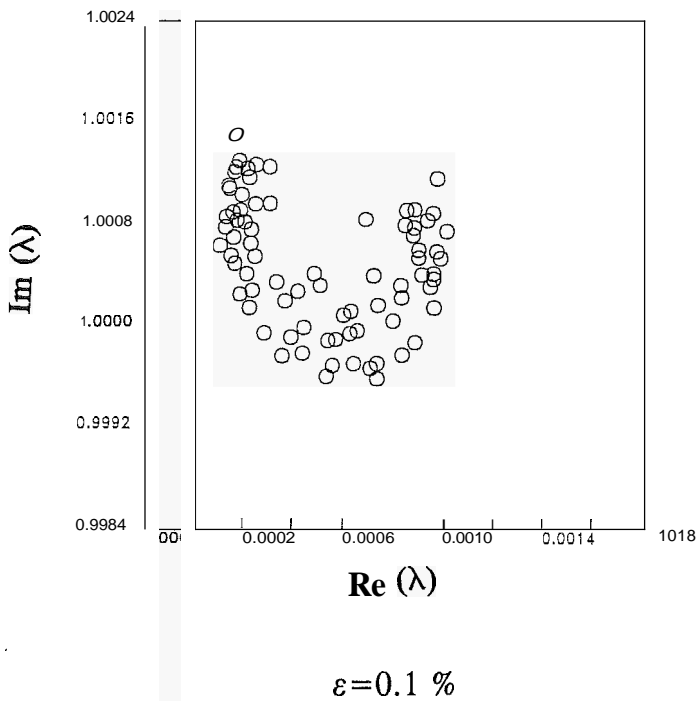
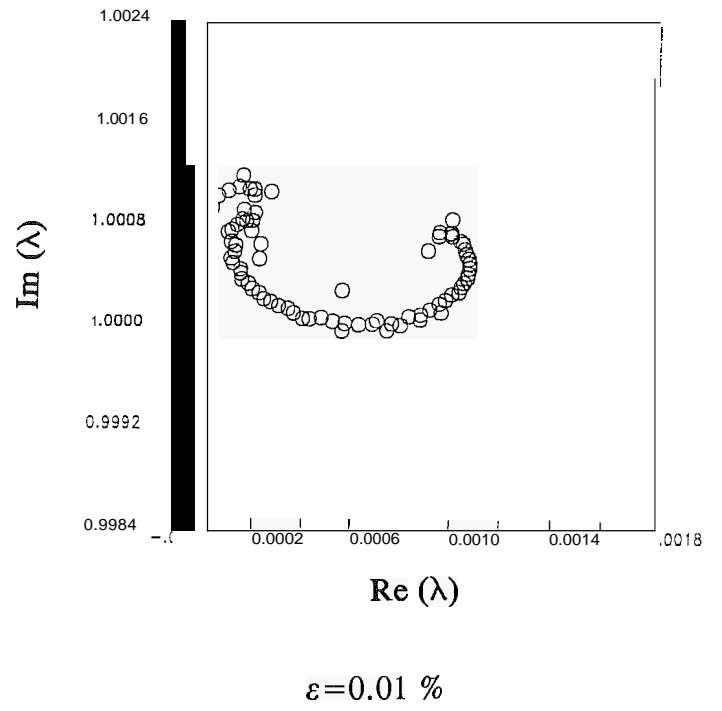
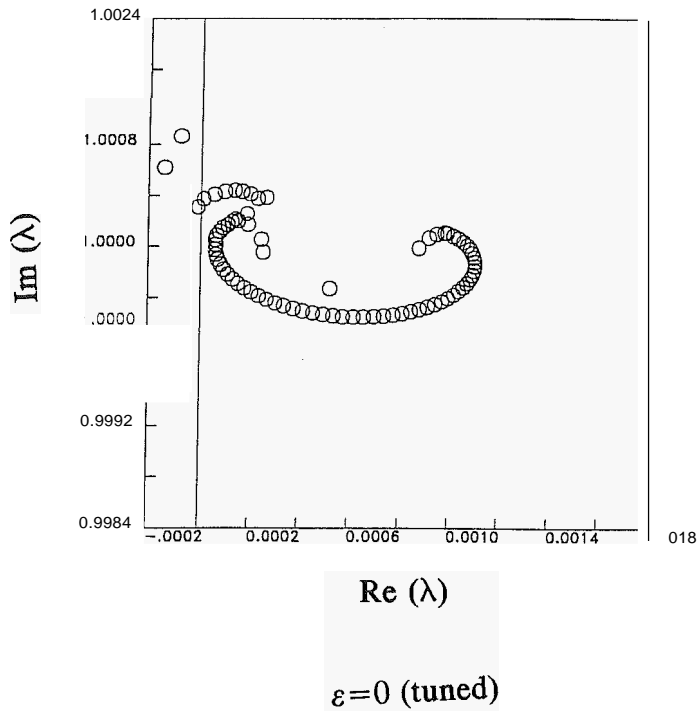


Figure 2. Root locus, in the complex plane, of the 78 aeroelastic eigenvalues in the edgewise mode group, for various values of blade mistuning.

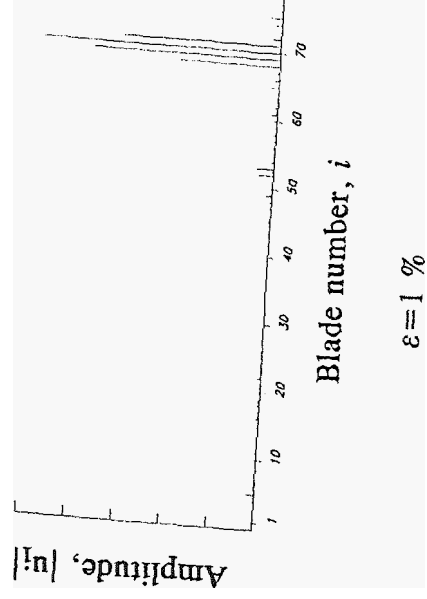
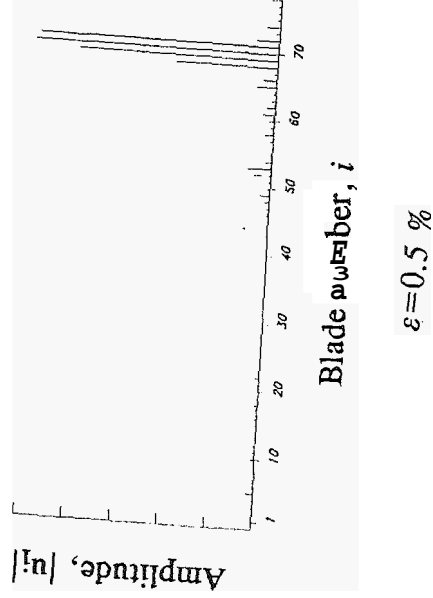
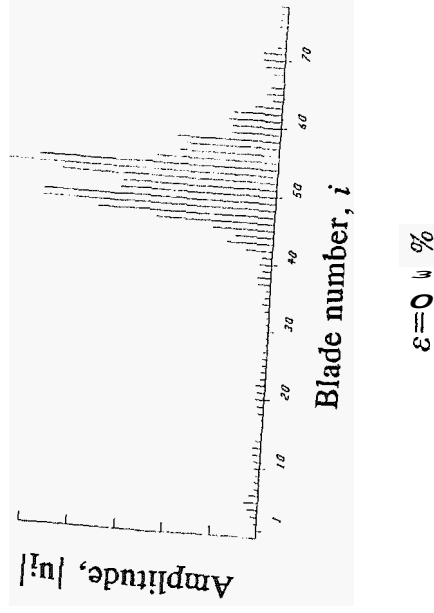
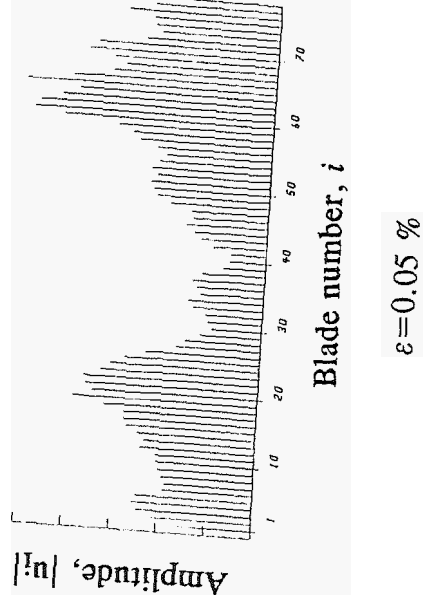
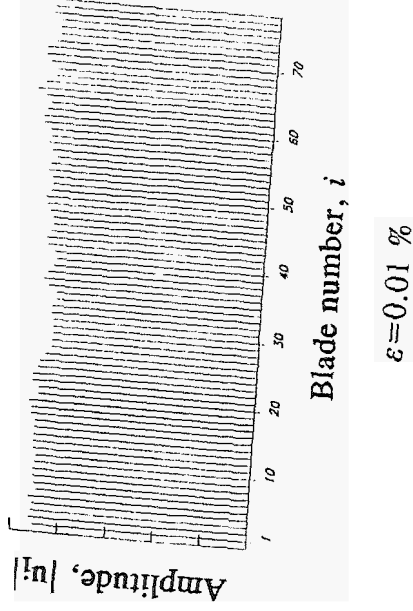
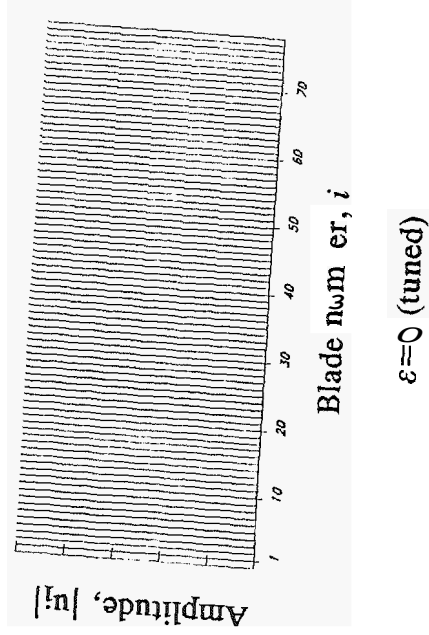
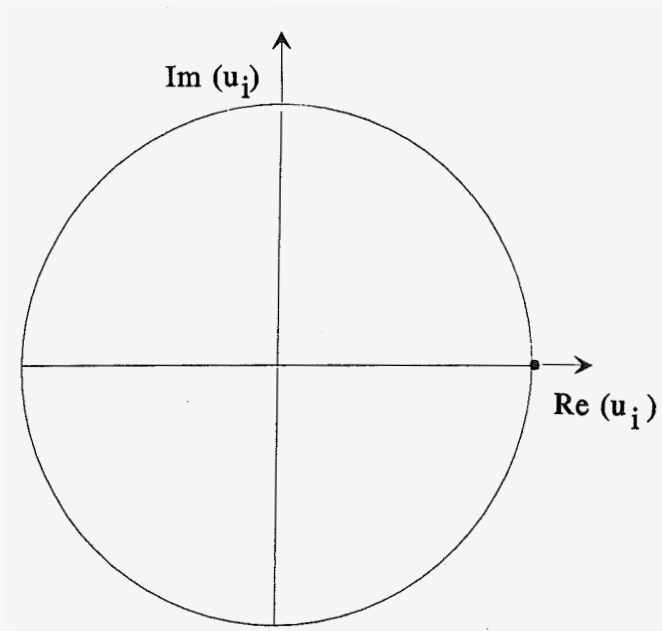
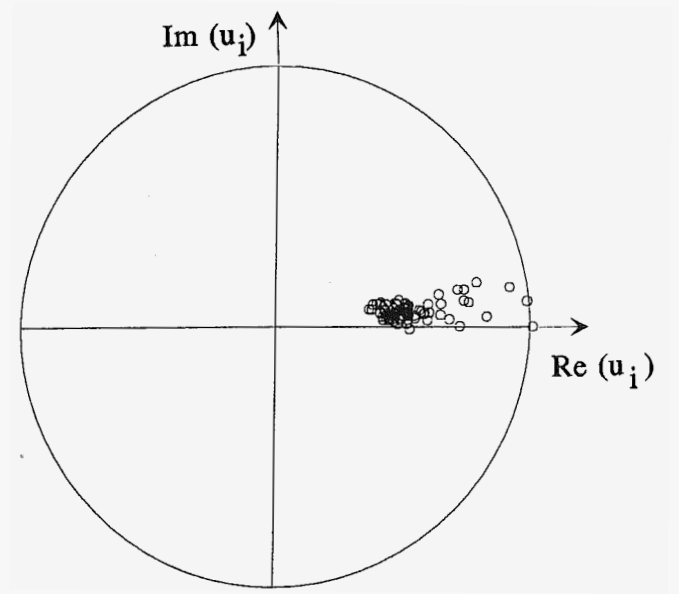


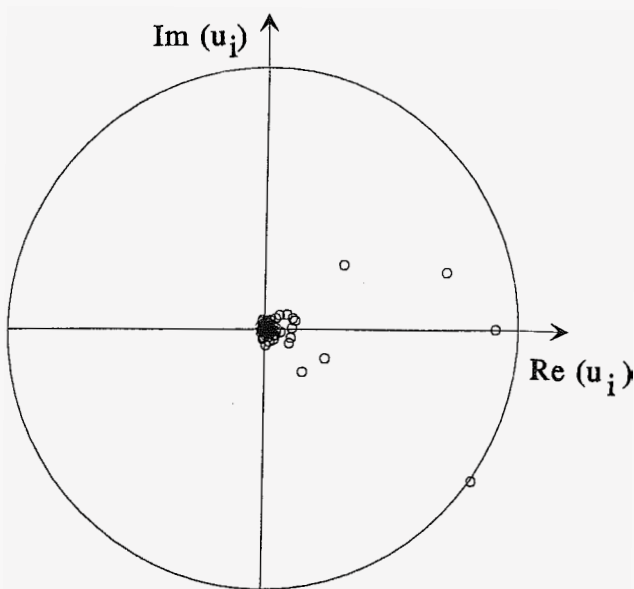
Figure 3. Amplitude pattern of the aeroelastic mode shape associated with the most unstable eigenvalue in the edgewise mode group, for various mistuning strengths.



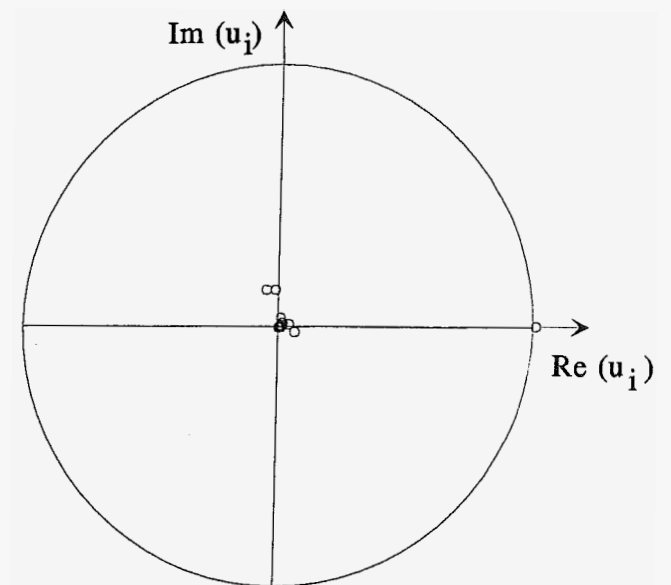
$\varepsilon=0$ (tuned)



$\varepsilon=0.01\%$



$\varepsilon=0.1\%$



$\varepsilon=1\%$

Figure 4. Polar plot (imaginary versus real part) of the mode shape associated with the highest frequency eigenvalue in the edgewise mode group, for various values of blade mistuning.

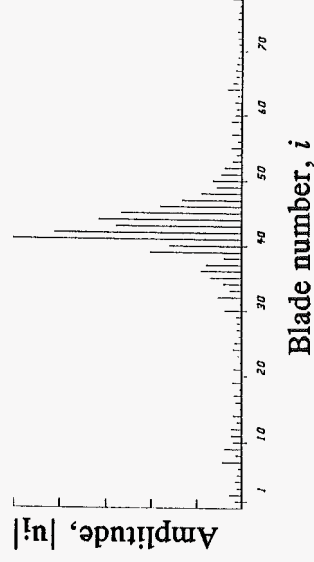
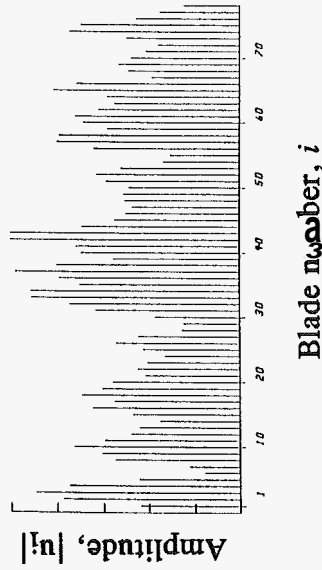
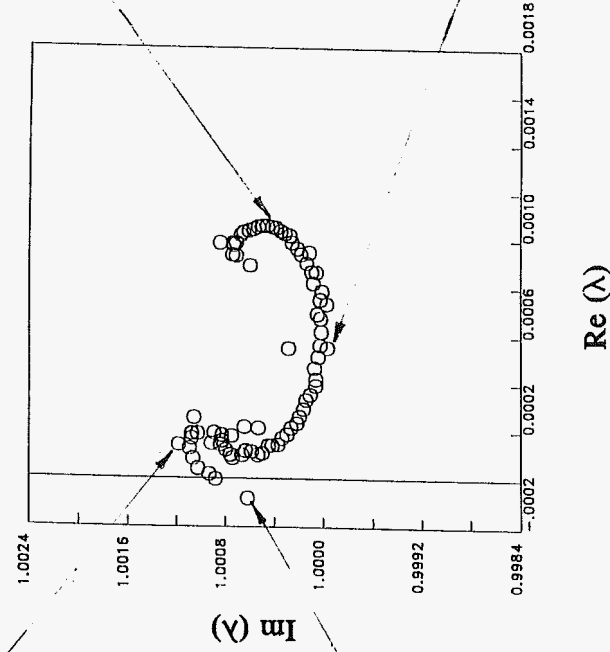
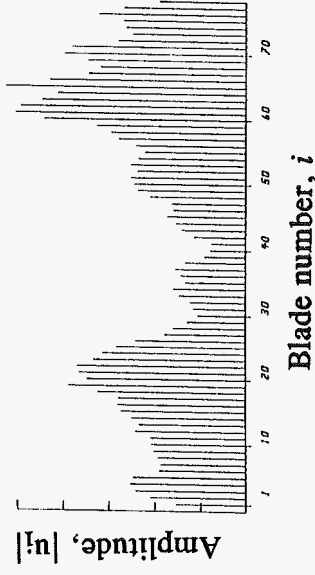
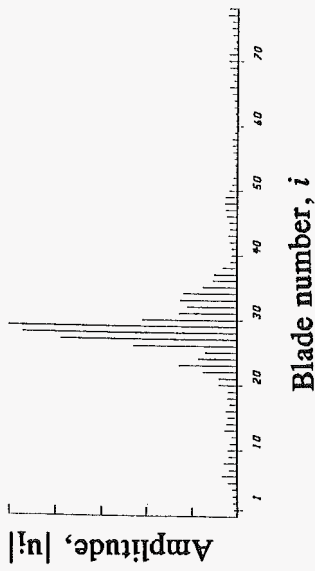


Figure 5. Amplitude patterns of selected aeroelastic mode shapes of an assembly with $\epsilon=0.05\%$ mistuning are shown on the associated root locus for the edgewise mode group. The lowest and highest frequency modes and the least and most stable modes are displayed.

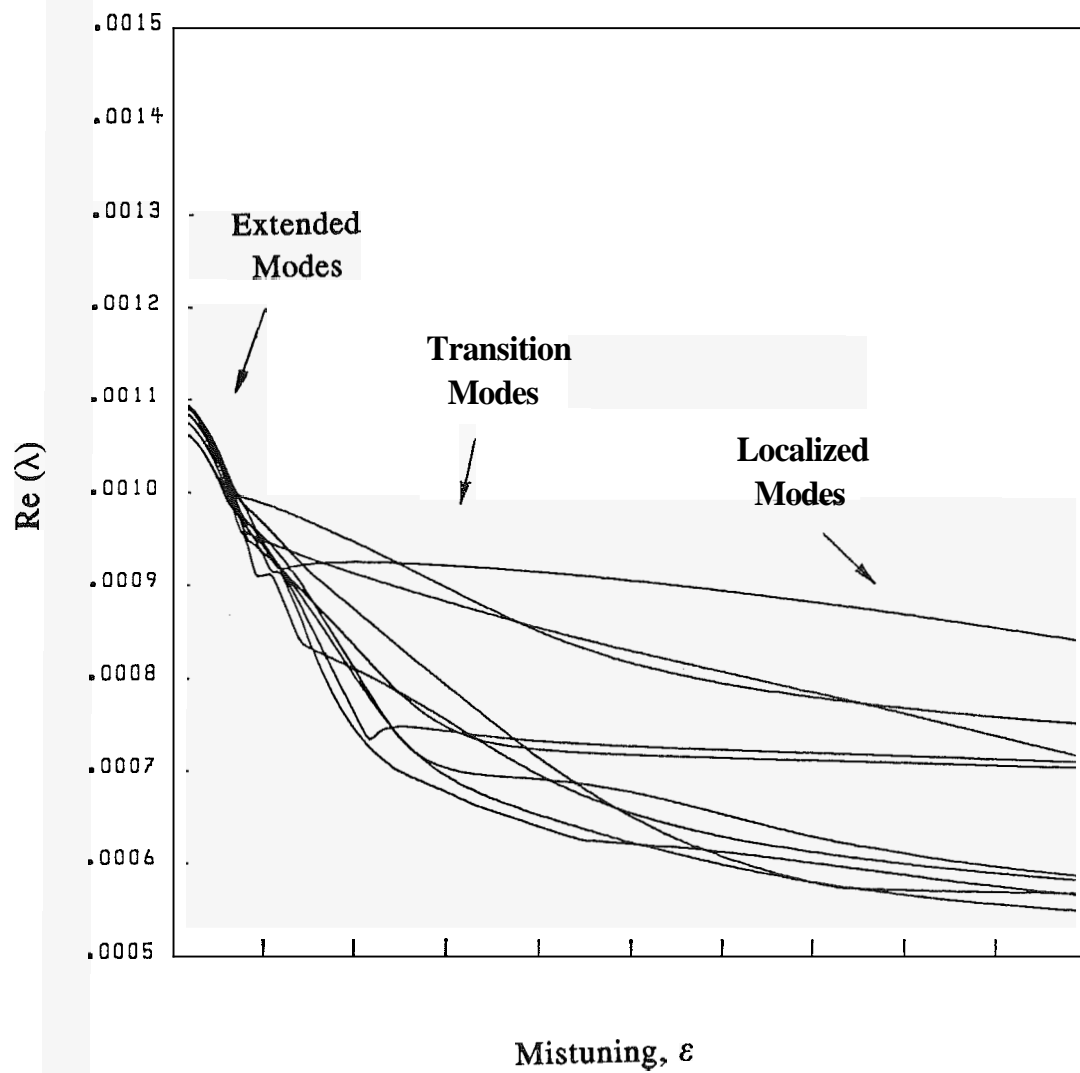


Figure 6. Loci of the real parts of the ten least stable eigenvalues in the edgewise mode group, versus mistuning standard deviation.

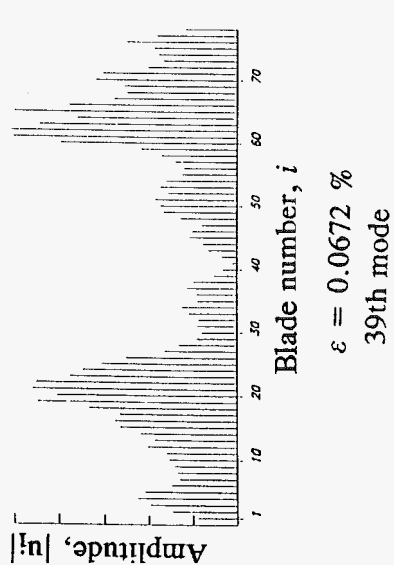
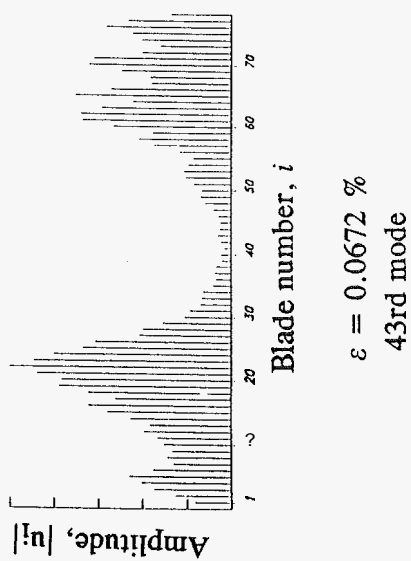
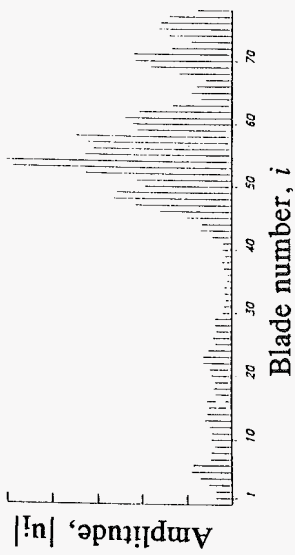
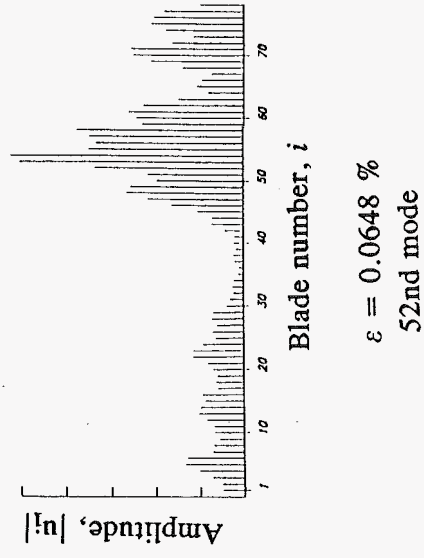
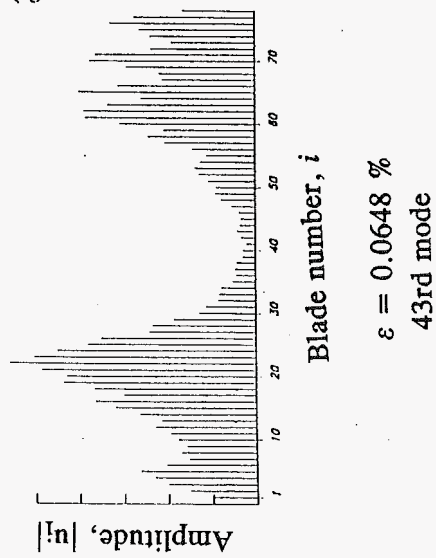
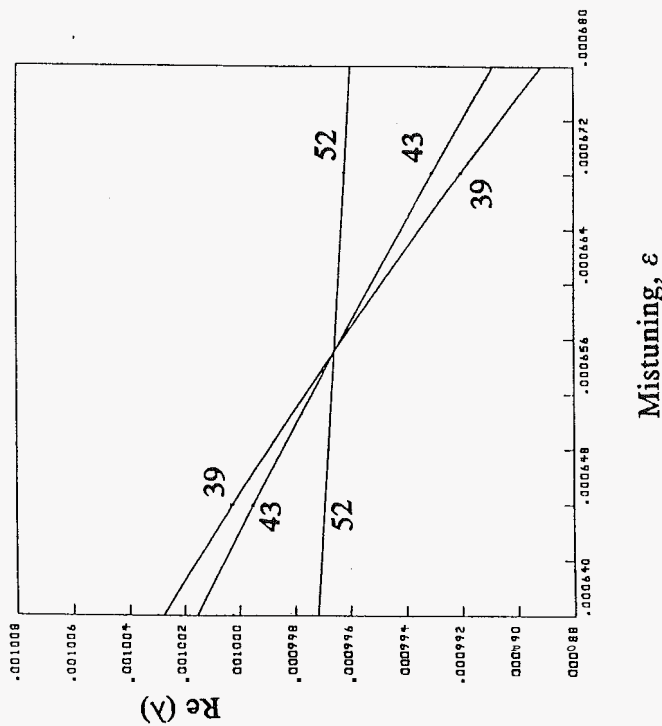
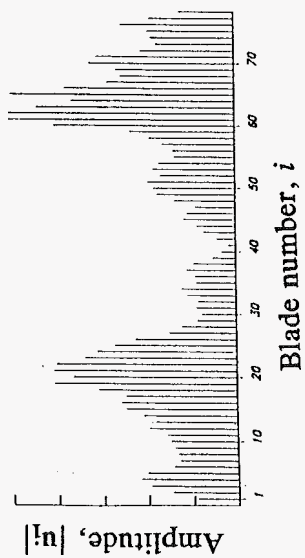


Figure 7. Crossing of three eigenvalue loci in a small mistuning range (enlargement of Figure 6). The associated mode shapes before and after the crossing are shown.

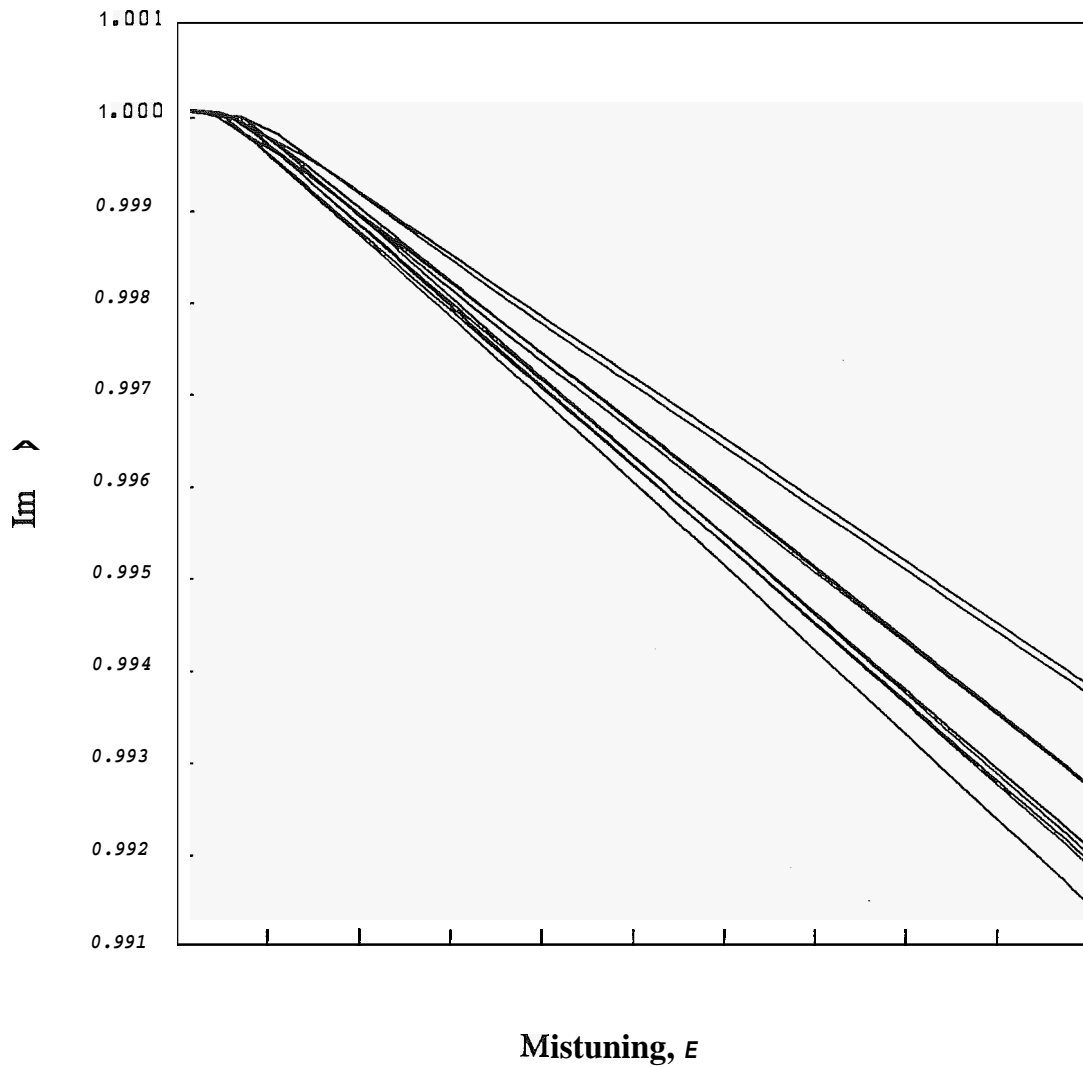
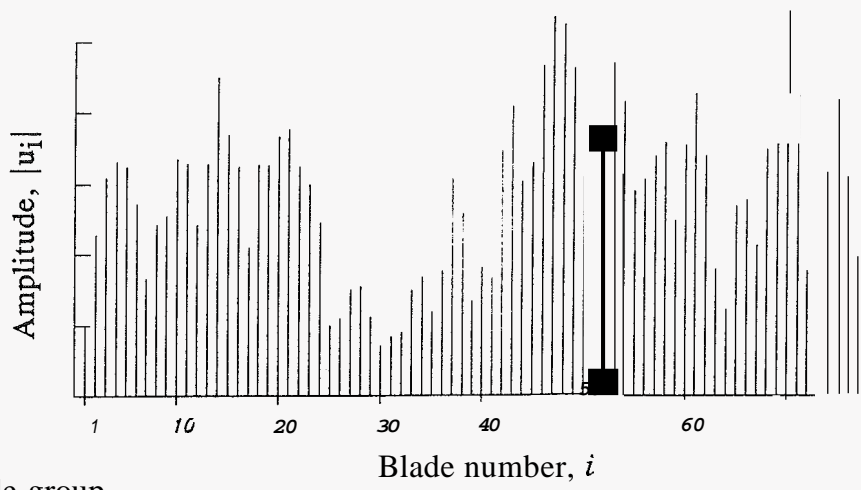
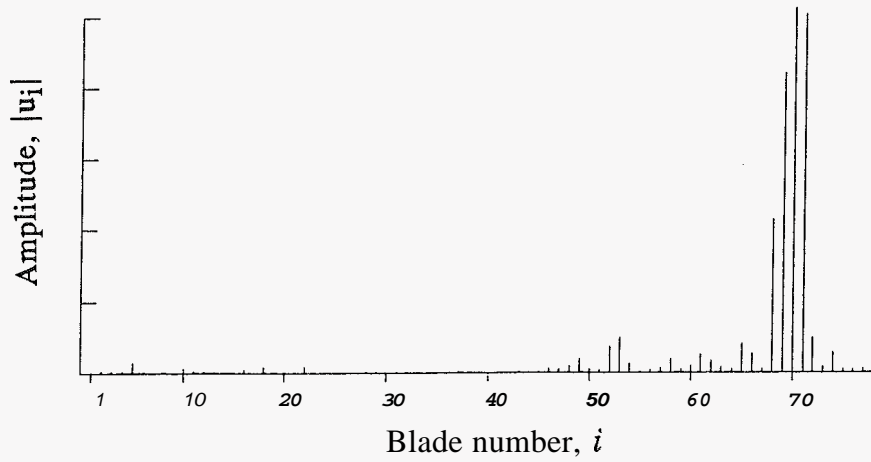


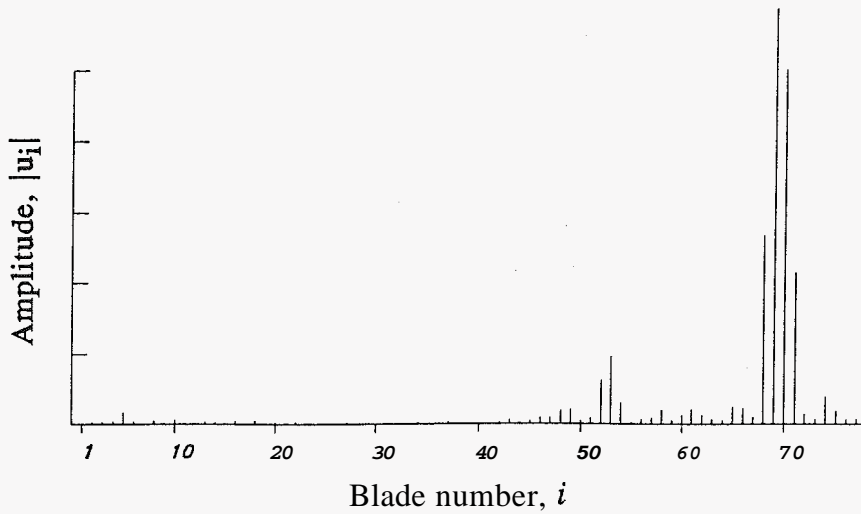
Figure 8. Loci of the imaginary parts of the ten lowest frequency eigenvalues in the edgewise mode group, versus mistuning standard deviation.



Bending mode group



Edgewise mode group



Torsion mode group

Figure 9. Amplitude pattern of the least stable mode shape in each of the first three mode groups (bending, edgewise and torsion). In all cases the blade mistuning is $\varepsilon=0.5\%$.

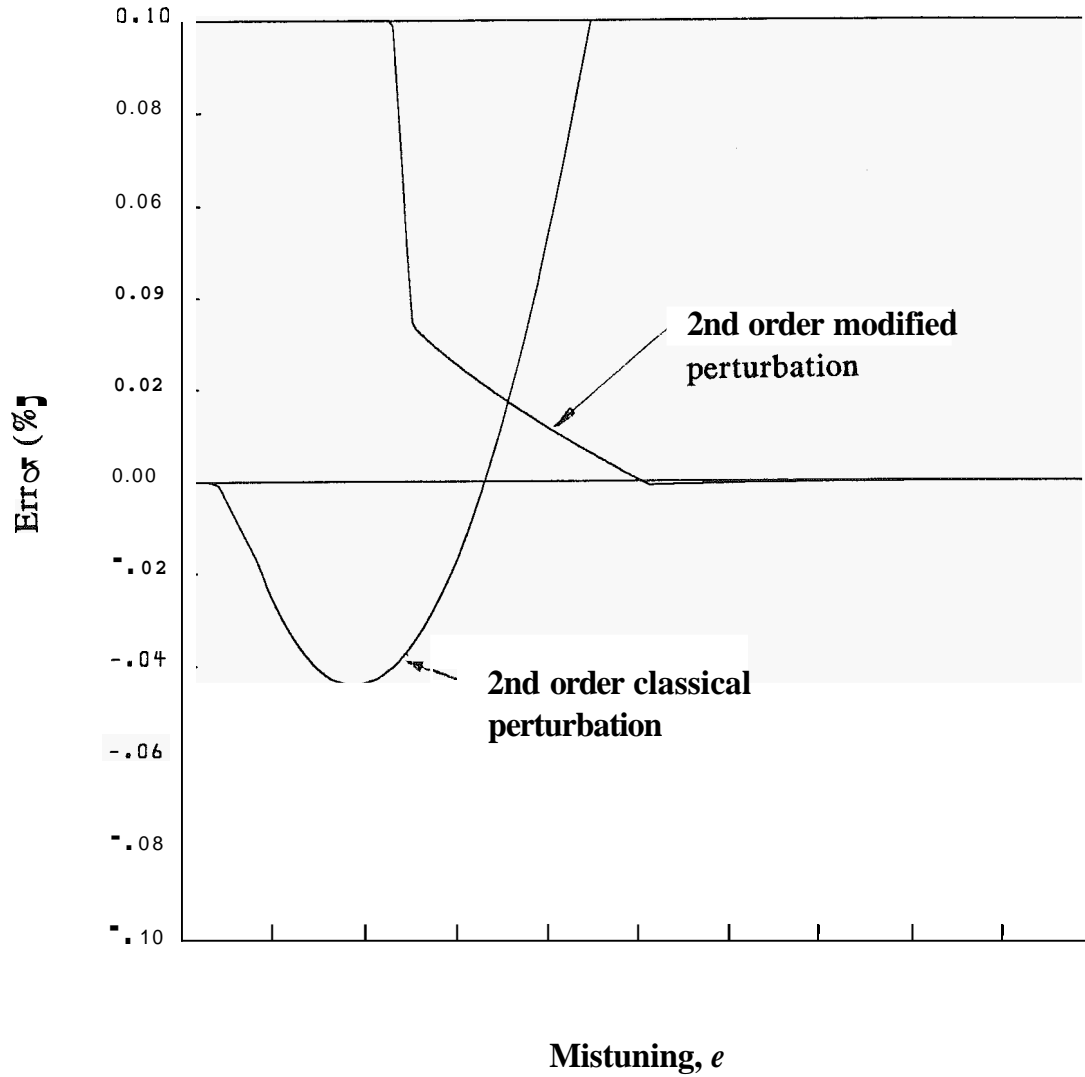


Figure 10. Comparison of the classical and modified perturbation results with the exact solution. The error from the exact solution is plotted versus the mistuning standard deviation, for the imaginary part of the lowest frequency eigenvalue in the edgewise mode group.

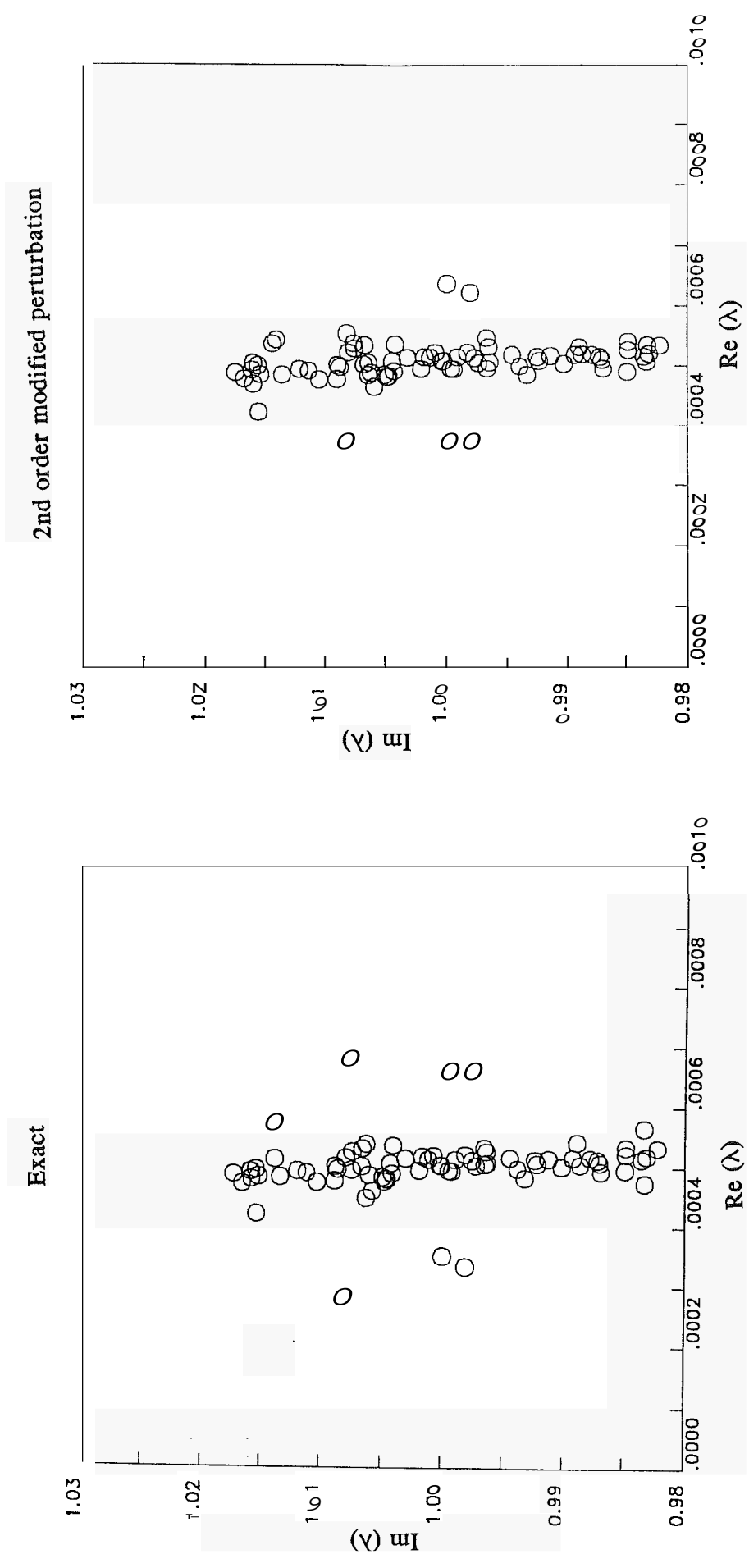


Figure 11. Root locus of the aeroelastic eigenvalues in the edgewise mode group, θ_y exact solution method and modified perturbation method. The mistuning is $\varepsilon=2\%$.

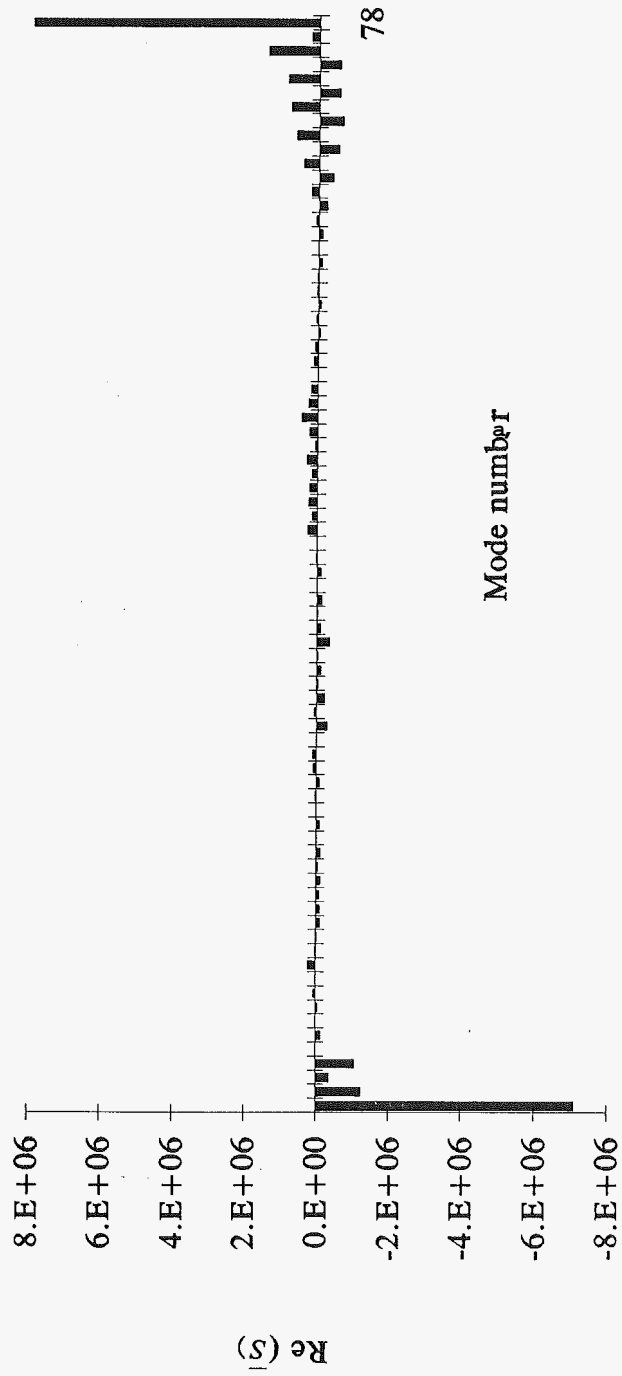


Figure 12. Real part of the stochastic sensitivity measure (representing the sensitivity of the frequencies) versus mode number. The modes are sorted from the lowest to the highest tuned frequency.

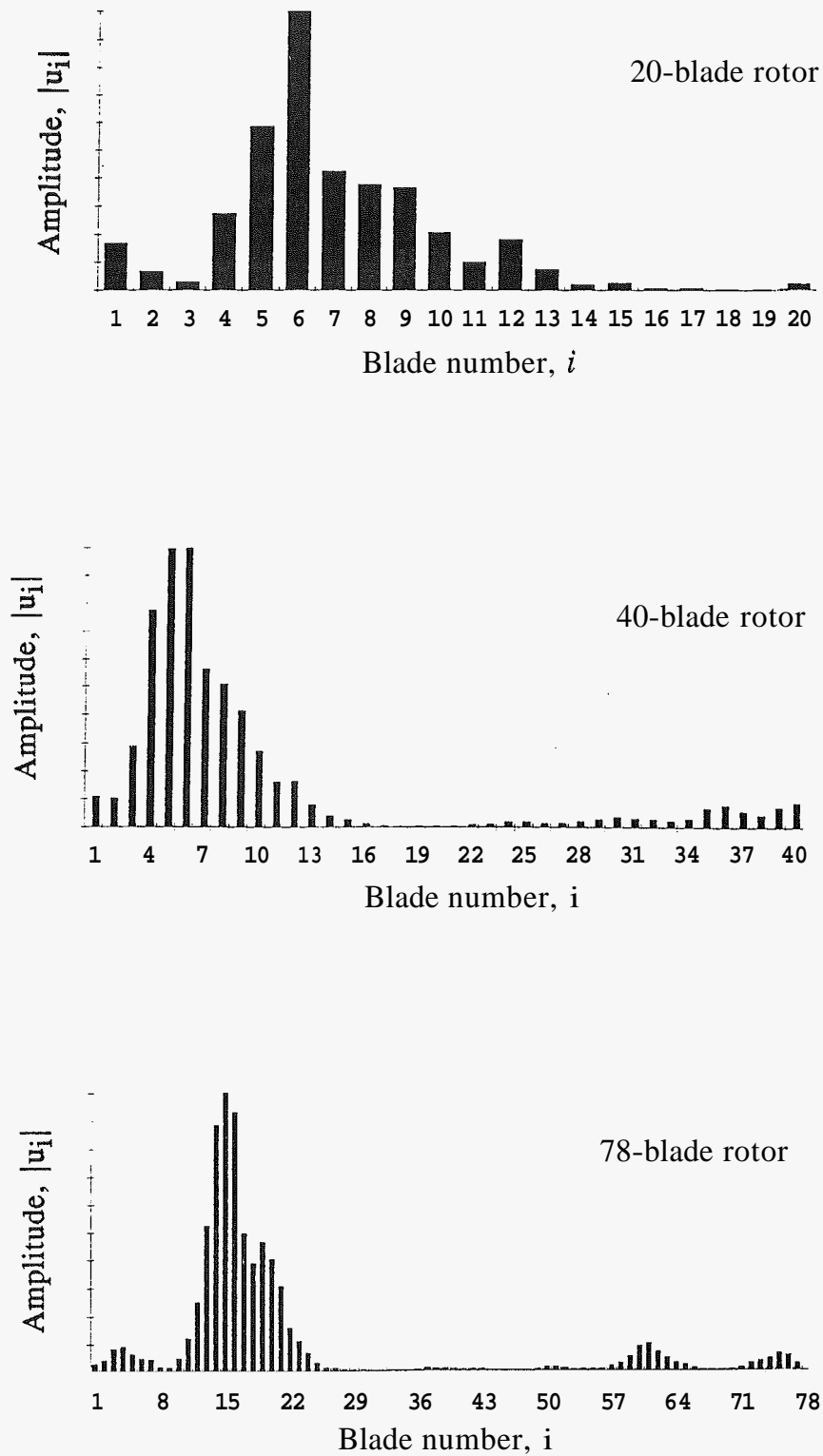


Figure 13. Amplitude pattern of the lowest frequency mode for various numbers of blades. In all cases the standard deviation of blade mistuning is $\varepsilon=0.63\%$.

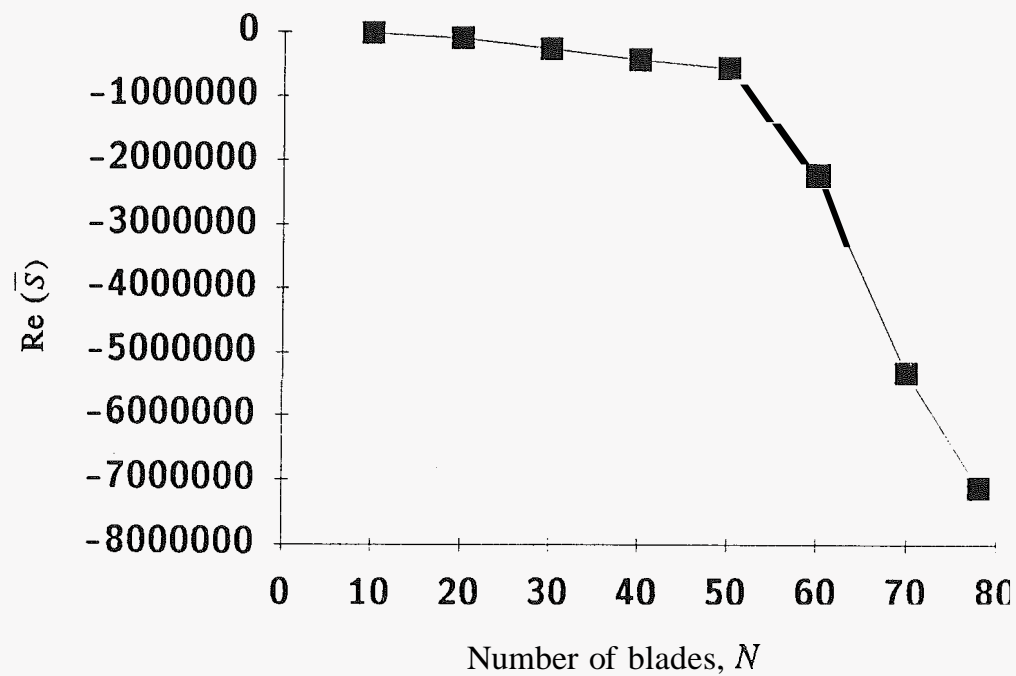


Figure 14. Real part of the sensitivity measure for the lowest frequency mode (representing the sensitivity of its frequency) versus the number of blades.



National Aeronautics and
Space Administration

Report Documentation Page

1. Report No. NASA TM - 104445 ICOMP-91-11; AIAA-91-3379		2. Government Accession No.		3. Recipient's Catalog No.	
4. Title and Subtitle Localization of Aeroelastic Modes in Mistuned High-Energy Turbines				5. Report Date	
				6. Performing Organization Code	
7. Author(s) Christophe Pierre, Todd E. Smith, and Durbha V. Murthy				8. Performing Organization Report No. E-6285	
				10. Work Unit No. 505-62-21	
9. Performing Organization Name and Address National Aeronautics and Space Administration Lewis Research Center Cleveland, Ohio 44135-3191				11. Contract or Grant No.	
				13. Type of Report and Period Covered Technical Memorandum	
12. Sponsoring Agency Name and Address National Aeronautics and Space Administration Washington, D.C. 20546-0001				14. Sponsoring Agency Code	
15. Supplementary Notes Prepared for the 27th Joint Propulsion Conference cosponsored by the AIAA , SAE, ASME, and ASEE, Sacramento, California, June 24-27, 1991. Christophe Pierre, The University of Michigan, Department of Mechanical Engineering and Applied Mechanics, Ann Arbor, Michigan 48109 (work funded by NASA Grant NAG3-1163) and Institute for Computational Mechanics in Propulsion, NASA Lewis Research Center (work funded by Space Act Agreement C-99066-G). Todd E. Smith, Sverdrup Technology, Inc., Lewis Research Center Group, 2001 Aerospace Parkway, Brook Park, Ohio 44142 (work funded by NASA Contract NAS3-25266). Durbha V. Murthy, the University of Toledo, Department of Mechanical Engineering, Toledo, Ohio 43606 and NASA Resident Research Associate at Lewis Research Center (work funded by NASA Grant NAG3-742). Space Act Monitor: Louis A. Povinelli (216) 433-5818.					
16. Abstract <p>The effects of blade mistuning on the aeroelastic vibration characteristics of high-energy turbines are investigated, using the first stage of the oxidizer turbopump in the space shuttle main rocket engine as an example. A modal aeroelastic analysis procedure is used in concert with a linearized unsteady aerodynamic theory that accounts for the effects of the blade thickness, camber, and steady loading. Extreme sensitivity of the dynamic characteristics of mistuned rotors is demonstrated. In particular, the aeroelastic modes become localized to a few blades, possibly leading to rogue blade failure, and the locus of the aeroelastic eigenvalues loses its structure when small mistuning (of the order present in actual rotors) is introduced. Perturbation analyses that yield physical insights into these phenomena are presented. A powerful but easily calculated stochastic sensitivity measure that allows the global prediction of mistuning effects is developed.</p>					
17. Key Words (Suggested by Author(s)) Space shuttle main engine Aeroelasticity Turbomachinery Mistuning			18. Distribution Statement Unclassified - Unlimited Subject Category 39		
19. Security Classif. (of the report) Unclassified		20. Security Classif. (of this page) Unclassified		21. No. of pages 36	22. Price* A03